Geological Magazine

www.cambridge.org/geo

Original Article

Cite this article: Bhatia H, Srivastava G, Adhikari P, Tao S, Utescher T, Paudayal KN, and Mehrotra RC (2022) Asian monsoon and vegetation shift: evidence from the Siwalik succession of India. *Geological Magazine* **159**: 1397–1414. https://doi.org/10.1017/S0016756822000243

Received: 6 September 2020
Revised: 16 March 2022
Accepted: 21 March 2022
First published online: 28 April 2022

Keywords:
climate change; C_4 plants; Coexistence Approach; Darjeeling; megafossils

Author for correspondence:
Gaurav Srivastava,
Email: gaurav_jan10@yahoo.co.in

© The Author(s), 2022. Published by Cambridge University Press.

Asian monsoon and vegetation shift: evidence from the Siwalik succession of India

Harshita Bhatia[1,2], Gaurav Srivastava[1,2], Purushottam Adhikari[3,4], Su Tao[5], Torsten Utescher[6,7], Khum N. Paudayal[3] and Rakesh C. Mehrotra[1]

[1]Birbal Sahni Institute of Palaeosciences, 53 University Road, Lucknow, 226 007, India; [2]Academy of Scientific and Innovative Research (AcSIR), Ghaziabad, 201002, India; [3]Central Department of Geology, Tribhuvan University, Kirtipur, Kathmandu, Nepal; [4]Department of Geology, Birendra Multiple Campus, Tribhuvan University, Bharatpur, Chitwan, Nepal; [5]CAS Key Laboratory of Tropical Forest Ecology, Xishuangbanna Tropical Botanical Garden, Chinese Academy of Sciences, Mengla, 666303, China; [6]Institute for Geosciences, University of Bonn, Bonn, Germany and [7]Senckenberg Research Institute, Frankfurt am Main, Germany

Abstract

Quantitative Miocene climate and vegetation data from the Siwalik succession of western Nepal indicate that the development of the Indian summer monsoon has had an impact, though in part, on vegetation changes. The climate and vegetation of the Lower (middle Miocene) and Middle (late Miocene–Pliocene) Siwalik successions of Darjeeling, eastern Himalaya, have been quantified. Reconstructed climate data, using the Coexistence Approach, suggest a decrease in winter temperatures and precipitation during the wettest months (MPwet) from the Lower to Middle Siwalik. The floristic assemblage suggests that Lower Siwalik forests were dominated by wet evergreen taxa, whereas deciduous ones became more dominant during the Middle Siwalik. The vegetation shift in the eastern Himalayan Siwalik was most likely due to a decrease in MPwet. The quantified climate–vegetation data from the eastern and western Himalayan Siwalik indicate that changes in the Indian summer monsoon had a profound impact on vegetation development during the period of deposition. We suggest that the decrease in winter temperature and summer monsoon rainfall during the Middle Siwalik might be linked with the Northern Hemisphere glaciation/cooling or a number of other things that were also going on at the time, including the continued rise of the Himalaya, and drying across the Tibetan region, which may have affected atmospheric circulation regionally.

1. Introduction

Globally, monsoon regions are mainly located in low latitude areas, which are subdivided into eight domains, namely the Indian Summer Monsoon (ISM), Western North Pacific Monsoon (WNPM), East Asia Monsoon (EAM), Indonesia–Australian Monsoon (I-AM), North America Monsoon (NAmM), South America Monsoon (SAmM), North Africa Monsoon (NAfM) and South Africa Monsoon (SAfM), depending on their location and characteristics (Yim *et al.* 2014; Wang *et al.* 2017). The ISM, EAM and WNPM are collectively known as the Asian Monsoon System that effects Asian climates and is considered the largest and strongest monsoon system on Earth (Wang *et al.* 2017). Basically, summer monsoons can be defined as the seasonal reversal of surface winds, and these reversals of seasonal winds are associated with rainy summers and dry winter seasons (Webster, 1987; Wang *et al.* 2017). The prediction of future South Asian monsoon behaviour in a warming world is complex, despite major advancements in understanding the variability of the ISM (Wang *et al.* 2015). The strength of the monsoon mainly depends on the land–ocean configuration, regional topography and insolation (Wang *et al.* 2017). The ISM is a topographically modified system (Boos & Kuang, 2010; Molnar *et al.* 2010; Ding *et al.* 2017), and the major heat source for the ISM to generate the temperature gradient between the land and ocean is located in the non-elevated part of northern India (Molnar *et al.* 2010; Boos & Kuang, 2013), while the Himalaya insulates this region from the cold and dry mid-latitude winds (Boos & Kuang, 2010; Acosta & Huber, 2020) (Fig. 1). In meteorology, monsoon characterization and monitoring is based on instrumental records of climatic parameters (Parthasarathy *et al.* 1992; Liu & Yin, 2002; Zhang & Wang, 2008; Zhao *et al.* 2009) or atmospheric circulation (Goswami *et al.* 1999; Wang & Fan, 1999) primarily to understand the short-term temporal changes in monsoon behaviour. However, understanding deep time monsoon features from geological records is complicated and modern meteorological indices are not applicable. For deep time monsoonal climate characterization, different proxies such as isotopes and terrestrial fossils (animals and plants), often combined with climate modelling, have been used to understand its behaviour (Clift *et al.* 2008, 2020; Srivastava *et al.* 2018; Farnsworth *et al.* 2019; Bhatia *et al.* 2021*a*,*b*) and thus have to use different criteria to define monsoon patterns. Typically, geological proxies use estimates of rainfall to understand monsoon fluctuations

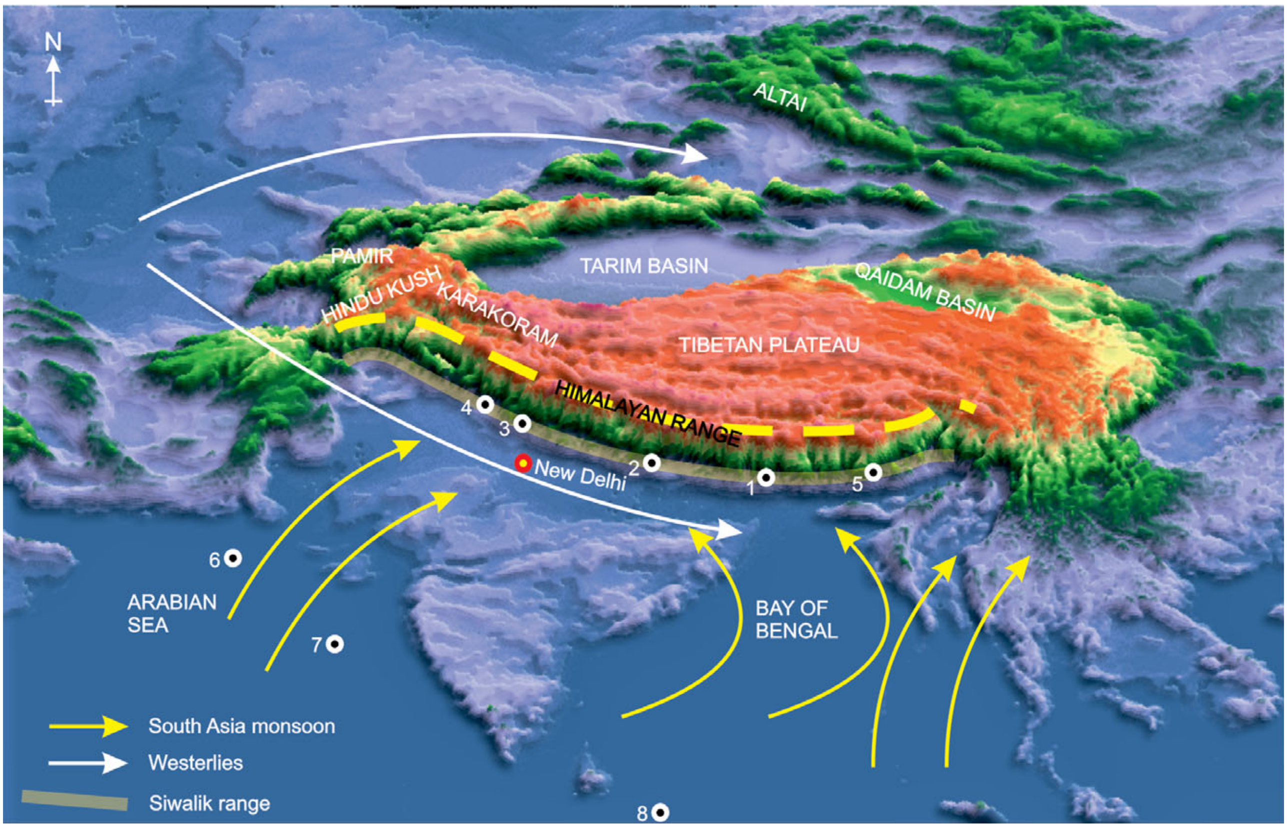

Fig. 1. (Colour online) Physiographic map showing the present fossil locality and previously studied sites: 1 – Darjeeling Siwalik, India; 2 – Surai Khola, Nepal (Hoorn *et al.* 2000); 3, 4 – Himachal Pradesh, India (Sanyal *et al.* 2004); 5 – Arunachal Pradesh Siwalik, India; 6 – Indus marine A-1, Arabian Sea (Clift *et al.* 2008); 7 – IODP site 1456, eastern Arabian Sea (Clift *et al.* 2020); 8 – ODP site 718, southern Bay of Bengal (Clift *et al.* 2008).

(Sanyal *et al.* 2004, 2005; Clift *et al.* 2008, 2020; Farnsworth *et al.* 2019), while plant proxies use either seasonal rainfall data (Ding *et al.* 2017; Srivastava *et al.* 2018) or integrated climate variable data as derived from leaf physiognomy (Spicer *et al.* 2016; Bhatia *et al.* 2021*a*,*b*) to understand monsoon presence.

In the central and western Himalayan Foreland Basin, isotopic studies indicate that a vegetation shift from C_3 to C_4 photosynthesis is linked with an increase in the seasonality of rainfall during late Miocene time (Quade *et al.* 1989, 1995; Sanyal *et al.* 2004, 2010). Moreover, recent data also suggest that winter precipitation caused by the western disturbances (WDs) and increase in frequency of forest fires also played an important role in providing positive feedback for this vegetation shift (Vögeli *et al.* 2017; Karp *et al.* 2018, 2021; Srivastava *et al.* 2018).

Quantitative palaeoclimate data using the Climate Leaf Analysis Multivariate Program (CLAMP) and Coexistence Approach (CA) on two palaeofloras retrieved from the Lower (middle Miocene: ~13–11 Ma) and Middle (late Miocene: 9.5–6.8 Ma) Siwalik succession of the western Himalaya, Nepal, indicate an increasing trend in mean annual temperature and cold month mean temperature throughout this interval, while the warm month mean temperature remained the same (Srivastava *et al.* 2018; Bhatia *et al.* 2021*b*). Moreover, rainfall data reveal that the ratio of summer to winter season precipitation increased from 3.47:1 to 9.16:1 (Srivastava *et al.* 2018). However, quantitative climate data from the Lower (13–10.5 Ma) and Middle (10.5–2.6 Ma) Siwalik climate of Arunachal Pradesh (Fig. 1) in the eastern Himalaya using CLAMP analysis indicate a decreasing trend in the mean annual temperature and cold month mean temperature, while the warm month mean temperature remained nearly the same.

The CLAMP methodology is independent of taxonomy and utilizes the relationship between dicot leaf morphological traits and their prevailing climatic conditions (Yang *et al.* 2015; Spicer *et al.* 2021). In angiosperms, dicot leaves are directly exposed to their immediate prevailing climatic conditions, and evolutionary selection means they are tuned for maximizing photosynthetic performance against resource investment, and this includes optimizing transpiration and leaf mechanics (Givnish, 1984; Pigliucci, 2003; Juenger *et al.* 2005; Rodriguez *et al.* 2014). Because of this, dicot leaves display distinctive physiognomic/morphological trait spectra reflective of the prevailing local climate (Spicer *et al.* 2021). However, CLAMP has some limitations as it can only be applied to dicot fossil leaves and requires a minimum of 20 different leaf morphotypes (Wolfe, 1993; Yang *et al.* 2015). Although CLAMP is robust in reconstructing the temperature-related climate variables, it however bears large uncertainties for rainfall prediction, because leaf forms are weakly constrained in wet regimes (Khan *et al.* 2014). In comparison, the CA can be applied to any fossil assemblages having leaves, wood, flowers, fruits and pollen, requires a minimum of ten taxa and is based on the nearest living relative (NLR) approach (Mosbrugger & Utescher, 1997; Utescher *et al.* 2014). The CA has a similar bias, to some extent, as that of CLAMP where water-loving taxa may be preferentially more represented near water bodies that provide the conditions for fossilization.

The quantitative palaeoclimate estimations derived from CLAMP and CA indicate that in each region different forcing factors were responsible for climate and vegetation changes. Isotopic, palynological and phytolith data from different sites within the central and western Himalayan Foreland Basin, marine sites from the Arabian Sea, Bay of Bengal and South China Sea, and the northern part of China indicate an overall decreasing trend in annual moisture and temperature, particularly after middle Miocene time (Quade *et al.* 1989, 1995; Hoorn *et al.* 2000; Ohja *et al.* 2000; Sanyal *et al.* 2004; Clift *et al.* 2008; Qin *et al.* 2011; Miao *et al.* 2012, 2017; Wang *et al.* 2019) (Fig. 1), and this change was most likely linked to the Northern Hemisphere glaciation/global cooling (Zachos *et al.* 2001, 2008). However, a recent study based on climate modelling and data comparison for eastern Asia shows an increase in overall rainfall up to Pliocene time due to the development of a 'supermonsoon' (Farnsworth *et al.* 2019).

The NE region of India is surrounded by mountains in the north, east and south with hills within the region and an opening to the west to receive moisture transported by the westerlies (Fig. 1). This region receives most of the rainfall (~151.3 cm) during the monsoon season, a considerably larger amount than the all-India average rainfall (86.5 cm) (Parthasarathy *et al.* 1995). Moreover, the monthly variability of rainfall during the summer monsoon season is also low (Parthasarathy & Dhar, 1974). Besides this, the NE region receives a significant amount of rainfall (~25 % of its annual total) during the pre-monsoon season (March–May/MAM), related to thunderstorms (Mahanta *et al.* 2013). The pre-monsoon (March–May/MAM) rainfall is a local convective rainfall, while summer monsoon (June–September/JJAS) rainfall is mainly delivered by large-scale summer monsoon circulation. Overall, the region receives 80 % of the annual rainfall during the pre-monsoon and summer monsoon seasons (Mahanta *et al.* 2013). Because of the unique hydrological setting of NE India, it is important to understand the evolution of such hydrological changes in the geological past. However, only a few attempts have been made to quantitatively reconstruct the hydrological changes in NE India (Tiwari *et al.* 2012; Khan *et al.* 2014; Srivastava *et al.* 2017). The CA has the ability to quantitatively reconstruct Neogene seasonal rainfall such as precipitation during the warmest months (MPwarm), which represents the pre-monsoon (March–May/MAM), and precipitation during the wettest months (MPwet), i.e. summer monsoon (June–September/JJAS) (Srivastava *et al.* 2017, 2018).

Here, using the CA, we quantitatively reconstruct the climate of the Lower (middle Miocene) and Middle (late Miocene–Pliocene) Siwalik successions based on the fossil megaflora of the Darjeeling district (Fig. 2), eastern Himalaya (Fig. 1). The reconstructed climate data will be helpful in understanding the changing patterns in climate (temperature, rainfall and summer monsoon strength), vegetation shifts and C_4 plant expansion during the Mio-Pliocene.

1.a. Geological setting of the study area

The deposition of muds, sands and gravels between the Lesser Himalaya in the north and the Gangetic Plains in the south since middle Miocene time was the product of ancient rivers draining from the active Himalayan orogeny. This sediment accumulation took place all along the length of the Himalayan Foreland Basin covering a longitudinal distance of ~2400 km and attaining a thickness of ~6 km (Kumar *et al.* 2011; Jain *et al.* 2020) in a coarsening upward succession known as the Siwalik Group (Fig. 1). The Siwalik succession is divided into three sub-groups, namely the Lower, Middle and Upper Siwalik (Pilgrim, 1910, 1913). The sediments of the Lower Siwalik are characterized by an alternation of fine- to medium-grained sandstones and variegated mudstones and are interpreted to have been deposited by meandering river systems, while the Middle Siwalik sediments are marked by medium- to coarse-grained, grey, micaceous salt-and-pepper coloured sandstone and are interpreted to have been deposited by a braided fluvial system. The Upper Siwalik comprises pebble and cobble conglomerates and formed as alluvial fan deposits near the mountain front (Tandon, 1991; Chakraborty *et al.* 2020; Jain *et al.* 2020).

In Darjeeling, the Siwalik Group is represented by three formations, namely the Gish Clay, Geabdat Sandstone and Parbu Grit, which are equivalent to the Lower, Middle and Upper Siwalik (Ganguly & Rao, 1970; Acharya, 1994) (Fig. 2). The Gish Clay Formation is characterized by medium- to fine-grained, well-sorted sandstones, subordinate micaceous sandstones, bluish nodular silty shale and claystone, while the Geabdat Sandstone Formation bears weakly indurated, medium- to coarse-grained salt-and-pepper coloured sandstones. Calcareous concretions of various shapes and sizes are also present. The Parbu Grit Formation is characterized by pebbly sandstone and coarse to medium sandstone (Ganguly & Rao, 1970; Acharyya, 1994; Matin & Mukul, 2010; Khan *et al.* 2014) (Table 1). Abundant plant fossils are present in the Gish Clay and Geabdat Sandstone formations (Fig. 3).

1.b. Age and depositional environment of the study area

In Darjeeling, based on the lithostratigraphy, the age of the Lower and Middle Siwalik is assigned to the middle–late Miocene and Pliocene, respectively (Ganguly & Rao, 1970; Acharyya, 1994; Khan *et al.* 2014). Furthermore, the dominance of characteristic leaf megafossils (such as *Shorea* sp., *Albizia* sp. and *Acacia* sp.) and invertebrate (*Globigerenoides* sp.) fossil assemblages suggest a depositional period of between middle Miocene and Pliocene in the Tista valley of the Darjeeling Siwalik (Acharyya *et al.* 1979; D. K. Paruya, unpub. Ph.D. thesis, Univ. Calcutta, 2012; Khan *et al.* 2016; More *et al.* 2018). However, recent works based on lithostratigraphy, magnetostratigraphy and sub-basin correlation assigned the age of the Lower (Gish Clay Formation) and Middle (Geabdat Sandstone Formation) Siwalik of Darjeeling to the middle Miocene and late Miocene–Pliocene, respectively (Acharyya, 1994; Taral *et al.* 2017; Taral & Chakraborty, 2018; Chakraborty *et al.* 2020; Roy *et al.* 2021).

It has been observed that the depositional environment of the eastern Siwalik differed from that of the western and central Siwalik. The sediments of the western and central regions are exclusively terrestrial and were deposited by meandering and braided rivers (DeCelles *et al.* 1998; Nakayama & Ulak, 1999; Kumar *et al.* 2003*a*,*b*, 2011). However, the depositional environment of the eastern Siwalik has some marine influence (Mitra *et al.* 2000; Chirouze *et al.* 2012; Coutand *et al.* 2016; More *et al.* 2016; Taral *et al.* 2017; Roy *et al.* 2021). This dissimilarity is referable to the fact that the eastern region of India was not connected to Eurasia in the way that the western and central regions were before middle Miocene time (Sinha *et al.* 1982; Ranga Rao, 1983). This is due to the diachronous collision of the Indian Plate with the Eurasian Plate, which started from the west and progressed towards the east, and might have delayed the closure of marine incursions in the eastern Siwalik region (Rowley, 1996; Uddin & Lundberg, 2004; Yin, 2006; Acharyya, 2007).

In the Darjeeling Siwalik, the palynological assemblages recovered from the Geabdat Sandstone Formation of the Churanthi

https://doi.org/10.1017/S0016756822000243 Published online by Cambridge University Press

Table 1. The lithostratigraphy of the Siwalik Group in the Darjeeling–Sikkim Himalayan region (after Taral & Chakraborty, 2018)

Age	Generalized lithostratigraphy	Formation	Description
Pliocene	Upper Siwalik	Murti boulder bed	Crudely bedded, pebble-boulder conglomerate and pebble sandstone
		Parbu grit	Pebbly, coarse- to fine-grained sandstone with pebble conglomerate; minor mudstone
Late Miocene–Pliocene	Middle Siwalik	Geabdat sandstone	Medium- to coarse-grained sandstone; local pebble beds, mudstone and minor marl
Middle Miocene	Lower Siwalik	Gish/Chunabati Formation	Fine- to medium-grained sandstone, siltstone, grey to greenish grey mudstone; bedded and nodular marl

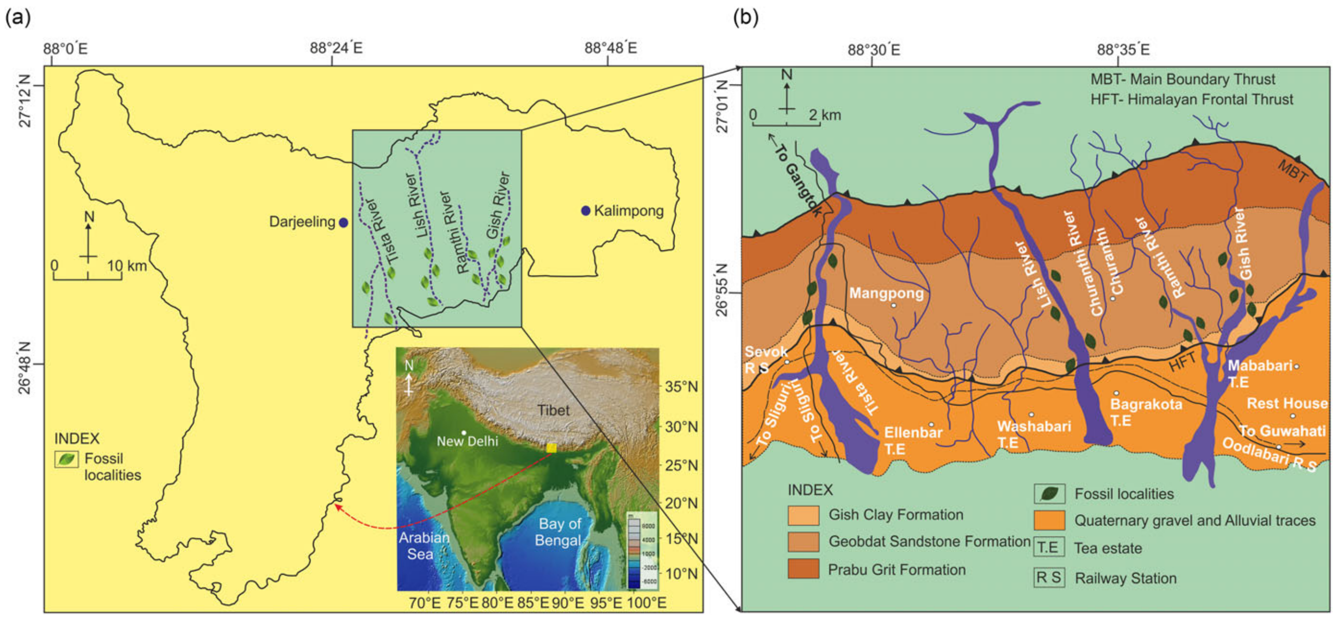

Fig. 2. (Colour online) Geological map of the fossil locality showing different formations and fossil localities (red asterisks) (modified after Prasad *et al.* 2015).

River section, which is 4 km west of the Gish River, include pollen grains of *Palaeosantalaceaepites* sp., *Zonocostites* sp. (Rhizophoraceae), *Malvacearumpollis* sp. (Malvaceae), *Araliaceoipollenites* (Araliaceae) and isolated salt glands of mangrove plant leaves (*Heliospermopsis siwalikii* and *Heliospermopsis* sp.) indicating the presence of brackish water in a possible nearshore marine environment (Mitra *et al.* 2000; More *et al.* 2016). Moreover, the sedimentary structure, vertical succession of strata, palaeocurrent patterns and characteristic trace fossils, such as *Cylindrichnus*, *Rosselia*, *Rhizocorallium*, *Chondrites* and *Zoophycos* reported from the Geabdat Sandstone Formation of the Tista valley, strongly suggest a marine deltaic environment (Taral *et al.* 2017). Additionally, characteristic biomarkers derived from organic matter from upper Miocene to Pliocene sediments of the Darjeeling Siwalik indicate, apart from the dominance of a terrestrial environment, substantial contributions from marine sources (Roy *et al.* 2021). Furthermore, sedimentology, plant megafossils and palynological analysis indicate a brackish or marginal marine deltaic environment in the Bhutan and Arunachal Pradesh Siwalik of NE India (Singh & Tripathi, 1990; Joshi *et al.* 2003; Chirouze *et al.* 2012; Coutand *et al.* 2016).

1.c. Modern climate of the fossil locality

The Darjeeling area has a sub-tropical to temperate/montane type of climate depending on elevation and aspect. The study site is located in the Oodlabari area of the Darjeeling district, West Bengal, and the present-day elevation of the area is ~200 m above sea level. The studied area is under the influence of a strong summer monsoon climate, where moisture is mostly sourced from the Bay of Bengal. The mean annual precipitation is 2047 mm, the mean precipitation during the wettest month is 1655 mm, the mean precipitation during the driest month is 38 mm, while the mean precipitation during the warmest month is 255 mm. The ratio of WET:DRY is 43.5 (India Meteorological Department, 1931–1960).

2. Materials and methods

In the present study, we use plant megafossils reported from the Lower and Middle Siwalik succession of the Darjeeling district. All fossils were collected from two formations, namely the Gish Clay (Lower Siwalik) and Geabdat Sandstone (Middle Siwalik)

https://doi.org/10.1017/S0016756822000243 Published online by Cambridge University Press

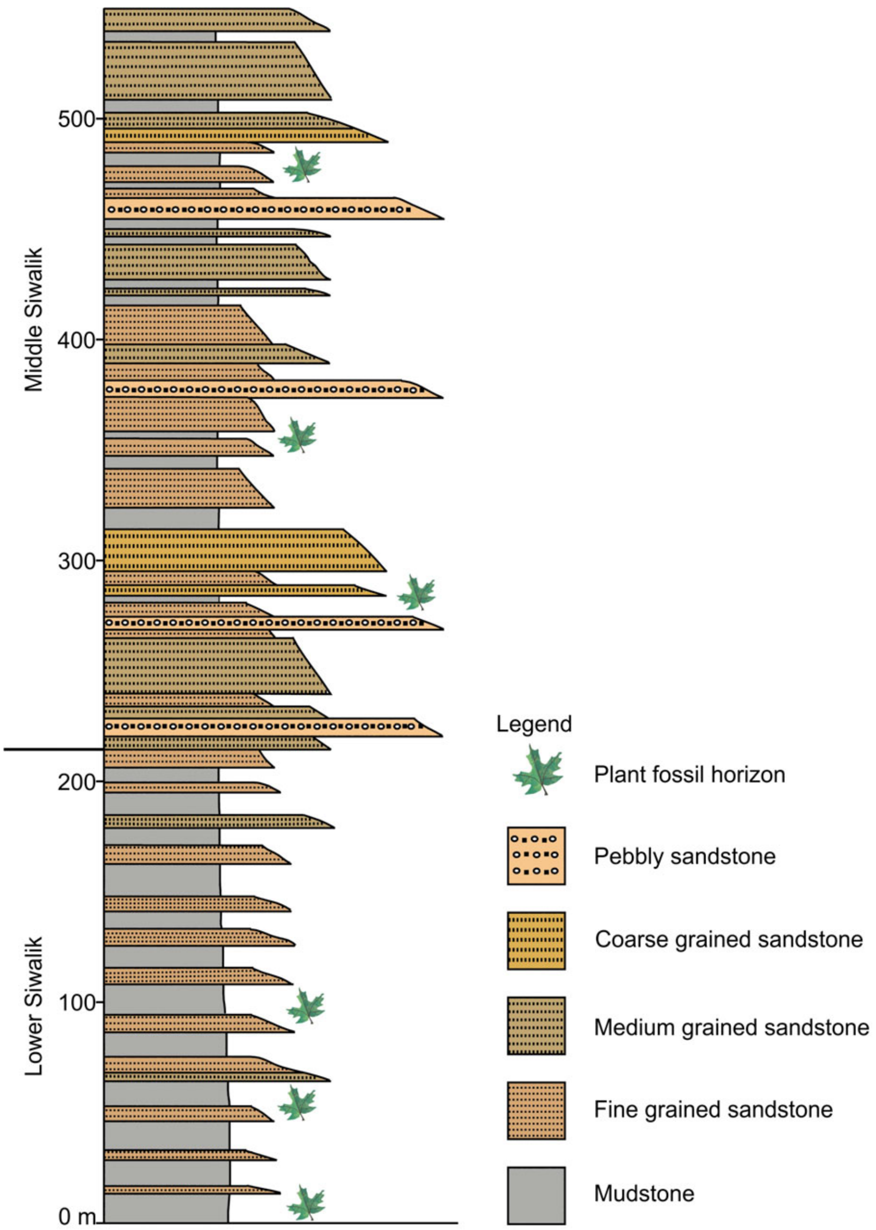

Fig. 3. (Colour online) Generalized lithology of the Lower and Middle Siwalik of the studied area (Darjeeling).

(Table 2; Figs 2, 3). The fossils were excavated from sedimentary rocks exposed near the rivers, namely the Ghish, Lish, Ramthi and Tista in the Oodlabari area of the Darjeeling district, West Bengal (Figs 2, 3) (Antal & Awasthi, 1993; Antal & Prasad, 1995, 1996*a*,*b*,*c*, 1997, 1998; Antal *et al.* 1996; Prasad *et al.* 2009, 2015).

In this study, we first identified the NLRs of all the fossil taxa and then segregated their habitats into the different forest types in which they are normally found. The forest types are classified according to their geographic, climatic and floristic traits that determine forest structure and composition (Champion & Seth, 1968; Rundel, 1999). A plant is considered evergreen when it bears leaves throughout the year, while deciduous ones are those that shed their leaves each year, particularly during the dry season (Champion & Seth, 1968).

The CA is used for the reconstruction of the Lower and Middle Siwalik climate of Darjeeling (Figs 1, 2). The CA is based on the philosophy of the NLR approach, which assumes that the modern analogues of the plant fossils have the same climatic tolerance as those of the fossils, and the technique can be applied to any fossil assemblage of leaves, wood, fruits, seeds and pollen. This methodology returns values consistent with those of other proxies for the Neogene to Quaternary periods where the majority of cases showed no significant change in the climatic requirement of any taxon (MacGinitie, 1941; Hickey, 1977; Chaloner & Creber, 1990; Mosbrugger, 1999). In this methodology, the fossils are first identified systematically and then the climatic tolerances of their modern analogues are obtained by documenting the climatic conditions of the area within which that taxon is found today. Thereafter, the coexistence interval can be determined by observing the maximum overlap of each climatic variable across the entire fossil assemblage composition. The observed coexistence intervals are considered, where climatic tolerances of the maximum taxa are

https://doi.org/10.1017/S0016756822000243 Published online by Cambridge University Press

Table 2. Fossil plants and their nearest living relatives (NLRs) from the Darjeeling Siwalik, West Bengal, India

Fossil taxa	Organ	NLRs	Numerical identifiers in Figures 7 & 9
Lower Siwalik			
Bauhinium palaeomalabaricum Prakash & Prasad	Wood	*Bauhinia* sp.	3
Beddomea palaeoindica Antal & Prasad	Leaf	Meliaceae	12
Bouea premacrophylla Antal & Awasthi	Leaf	Anacardiaceae	1
Cananga tertiara Prasad *et al.*	Leaf	Annonaceae	2
Casearia pretomentosa Antal & Awasthi	Leaf	*Casearia* sp.	4
Combretum sahnii Antal & Awasthi	Leaf	*Combretum* sp.	5
Glochidion palaeohirsutum Antal & Prasad	Leaf	Euphorbiaceae	7
Grewia tistaensis Antal & Prasad	Fruit	*Grewia* sp.	9
Homonoia mioriparia Antal & Prasad	Leaf	*Homonoia* sp.	10
Hopea kathgodamensis Prasad	Leaf	*Hopea* sp.	11
Millettia oodlabariensis Antal & Prasad	Leaf	*Millettia* sp.	13
Nothopegia eutravancorica Antal & Awasthi	Leaf	*Nothopegia* sp.	14
Paranephelium seriaensis Prasad & Dwivedi	Leaf	Sapindaceae	18
Polyalthia palaeosimiarum Awasthi & Prasad	Leaf	*Polyalthia* sp.	15
Pongamia siwalika Antal & Awasthi	Leaf	Fabaceae	8
Pterospermum siwalicum Antal & Prasad	Leaf	*Pterospermum* sp.	16
Shorea bengalensis Antal & Prasad	Leaf	*Shorea roxburghii*	6
Shorea siwalika Antal & Awasthi	Leaf	*Shorea* sp.	19
Swintonia miocenica Antal & Prasad	Leaf	*Swintonia* sp.	20
Syzygium palaeocuminii Prasad & Awasthi	Leaf	*Syzygium* sp.	21
Terminalia miobelerica Prasad	Leaf	*Terminalia* sp.	22
Uvaria ghishia Antal & Prasad	Leaf	*Uvaria* sp.	23
Ventilago tistaensis Antal & Prasad	Leaf	Rhamnaceae	17
Xanthophyllum mioflavescens Antal & Prasad	Leaf	*Xanthophyllum* sp.	24
Zizyphus palaeoapetala Antal & Prasad	Leaf	*Zizyphus* sp.	25
Middle Siwalik			
Actinodaphne palaeoangustifolia Antal & Awasthi	Leaf	*Actinodaphne* sp.	1
Albizia palaeolebbek Antal & Awasthi	Leaf	*Albizia* sp.	2
Alstonia mioscholaris Antal & Awasthi	Leaf	Apocynaceae	5
Bambusa sp.	Leaf	*Bambusa* sp.	6
Bauhinium palaeomalabaricum	Wood	*Bauhinia* sp.	7
Bombax palaeomalabaricum Prasad *et al.*	Leaf	*Bombax* sp.	8
Buchanania palaeosessilifolia Prasad *et al.*	Leaf	Anacardiaceae	3
Bursera preserrata Antal & Awasthi	Leaf	*Bursera* sp.	9
Calophyllum suraikholaensis Awasthi & Prasad	Leaf	*Calophyllum* sp.	10
Callicarpa siwalika Antal & Awasthi	Leaf	Verbenaceae	38
Chionanthus siwalicus Prasad *et al.*	Leaf	*Chionanthus* sp.	11
Cinnamomum sp.	Leaf	*Cinnamomum* sp.	12
Cupania oodlabariensis Prasad *et al.*	Leaf	*Cupania* sp.	13
Cynometra palaeoiripa Prasad *et al.*	Leaf	*Cynometra* sp.	14
Diospyros koilabasensis Prasad	Leaf	*Diospyros* sp.	15
Dipterocarpus siwalicus Lakhanpal & Guleria	Leaf	*Dipterocarpus* sp.	17

(*Continued*)

Table 2. (*Continued*)

Fossil taxa	Organ	NLRs	Numerical identifiers in Figures 7 & 9
Entada palaeoscandens Awasthi & Prasad	Seed	Fabaceae	18
Ficus oodlabariensis Antal & Awasthi	Fruit	*Ficus* sp.	19
Ficus retusoides Prasad	Leaf	Moraceae	28
Fissistigma senni Lakhanpal	Leaf	Annonaceae	4
Garcinia eocambogia Prasad	Leaf	*Garcinia* sp.	20
Gardenia precoronaria Prasad *et al.*	Leaf	*Gardenia* sp.	21
Grewia ghishia Antal & Awasthi	Leaf	*Grewia* sp.	22
Hopea siwalika Antal & Awasthi	Leaf	*Hopea* sp.	23
Lagerstroemia patelli Lakhanpal & Guleria	Leaf	*Lagerstroemia* sp.	24
Macaranga siwalika Antal & Awasthi	Leaf	*Macaranga* sp.	25
Mallotus kalimpongensis Antal & Awasthi	Leaf	*Mallotus* sp.	26
Millettia miosericea Prasad *et al.*	Leaf	*Millettia* sp.	27
Paranephelium miocenica Prasad *et al.*	Leaf	Sapindaceae	32
Pterospermum mioacerifolium Prasad *et al.*	Leaf	*Pterospermum* sp.	29
Rhamnus siwalicus Prasad *et al.*	Leaf	Rhamnaceae	30
Sabia eopaniculata Prasad	Leaf	*Sabia* sp.	31
Shorea miocenica Antal & Prasad	Leaf	*Shorea* sp.	33
Sterculia miocolorata Prasad *et al.*	Leaf	*Sterculia* sp.	34
Sterculia siwalica Prasad *et al.*	Leaf	Sterculiaceae	35
Toddalia miocenica Prasad *et al.*	Leaf	*Toddalia* sp.	36
Uvaria siwalica Prasad	Leaf	*Uvaria* sp.	37
Vatica siwalica Prasad *et al.*	Leaf	Dipterocarpaceae	16

included, as the most suitable ranges of different palaeoclimatic variables for a given fossil flora. The taxa which are present outside these coexistence intervals are considered outliers. Outliers result from many factors including wrong identification, imprecise climatic information for the modern analogues and a change in climatic tolerances through geologic time (Mosbrugger & Utescher, 1997; Utescher *et al.* 2014). The CA, like CLAMP, relies only on the presence/absence of taxa and is independent of sample size and relative abundance. CA reconstructions have been validated by other independent methodologies such as CLAMP (Liang *et al.* 2003; Uhl *et al.* 2007; Xing *et al.* 2012; Bondarenko *et al.* 2013). Generally, the CA results are also supported by oxygen isotope data retrieved from marine archives and palaeovegetational reconstruction (Mosbrugger *et al.* 2005; Utescher *et al.* 2015; Srivastava *et al.* 2016, 2018).

The CA reconstructs climatic variables such as mean annual temperature, cold month temperature, warm month temperature, mean annual precipitation, mean precipitation during the wettest months, mean precipitation during the driest months and mean precipitation during the warmest months. The climatic tolerances for all taxa in this study were obtained from the PALAEOFLORA database (Utescher & Mosbrugger, unpub. data, 2018: previously available at http://www.palaeoflora.de) (online Supplementary Material). The details of the PALAEOFLORA database and extraction of climate data for fossil NLRs are discussed by Utescher *et al.* (2014).

3. Results

3.a. Palaeofloristic analysis of the Lower and Middle Siwalik flora of Darjeeling

Modern analogues of the fossils reported from the Lower Siwalik succession belong to the families Anacardiaceae, Annonaceae, Combretaceae, Dipterocarpaceae, Euphorbiaceae, Fabaceae, Flacourtiaceae, Malvaceae, Meliaceae, Myrtaceae, Rhamnaceae, Rubiaceae, Sapindaceae and Xanthophyllaceae. A detailed list of taxa is provided in the online Supplementary Material. The most diverse plant families in the Lower Siwalik assemblage are: Flacourtiaceae and Fabaceae, followed by Anacardiaceae, Dipterocarpaceae, Combretaceae, Euphorbiaceae, Rhamnaceae, Meliaceae, Myrtaceae, Rubiaceae, Sapindaceae, Malvaceae, Tiliaceae and Xanthophyllaceae (Figs 4a, 5). The floristic assemblage suggests that 71 % of taxa are typically found in evergreen forests, whereas 19 % of taxa are typical of moist deciduous forests. However, only 10 % of taxa are evergreen to moist deciduous (Fig. 4b) (Champion & Seth, 1968).

Modern analogues of the fossils from the Middle Siwalik succession belong to families such as Anacardiaceae, Annonaceae, Apocynaceae, Bombacaceae, Burseraceae, Calophyllaceae, Clusiaceae, Compositae (Asteraceae), Dilleniaceae, Dipterocarpaceae, Ebenaceae, Euphorbiaceae, Fabaceae, Flacourtiaceae, Lauraceae, Lythraceae, Marantaceae, Moraceae, Oleaceae, Poaceae, Rhamnaceae, Rutaceae, Sabiaceae,

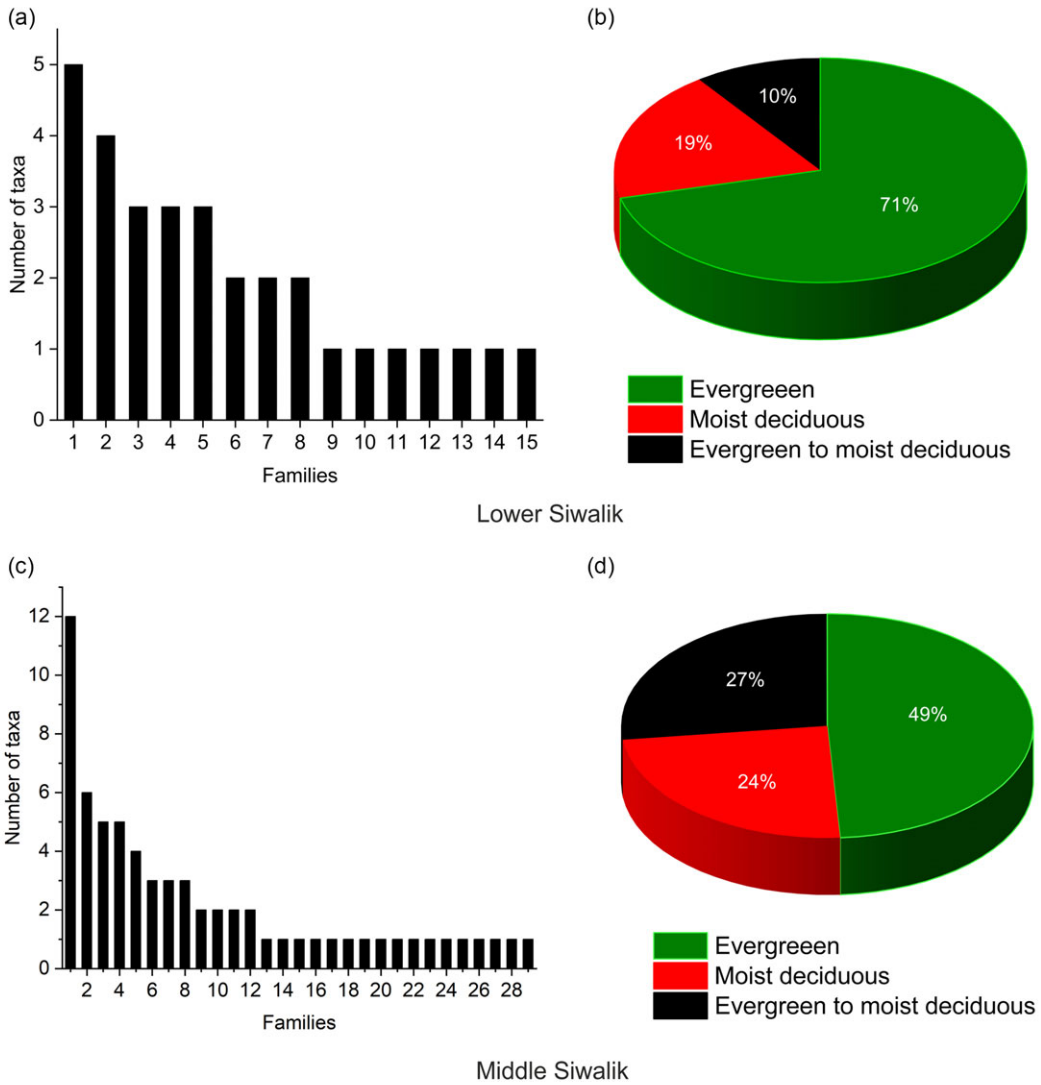

Fig. 4. (Colour online) (a–d) Bar and pie diagrams showing the floristic diversity and forest types during the Lower and Middle Siwalik of Darjeeling. (a) Floristic diversity during the Lower Siwalik. 1 – Flacourtiaceae; 2 – Fabaceae; 3 – Anacardiaceae; 4 – Annonaceae; 5 – Dipterocarpaceae; 6 – Combretaceae; 7 – Euphorbiaceae; 8 – Rhamnaceae; 9 – Meliaceae; 10 – Myrtaceae; 11 – Rubiaceae; 12 – Sapindaceae; 13 – Malvaceae; 14 – Tiliaceae; 15 – Xanthophyllaceae. (b) Pie diagram showing the forest types during the deposition of the Lower Siwalik sediments. (c) Floristic diversity during the Middle Siwalik. 1 – Fabaceae; 2 – Dipterocarpaceae; 3 – Annonaceae; 4 – Malvaceae; 5 – Sapindaceae; 6 – Apocynaceae; 7 – Flacourtiaceae; 8 – Moraceae; 9 – Burseraceae; 10 – Ebenaceae; 11 – Euphorbiaceae; 12 – Lauraceae; 13 – Anacardiaceae; 14 – Bombacaceae; 15 – Calophyllaceae; 16 – Clusiaceae; 17 – Compositae; 18 – Dilleniaceae; 19 – Lythraceae; 20 – Marantaceae; 21 – Oleaceae; 22 – Poaceae; 23 – Rhamnaceae; 24 – Rubiaceae; 25 – Rutaceae; 26 – Sabiaceae; 27 – Tiliaceae; 28 – Verbenaceae; 29 – Vitaceae. (d) Pie diagram showing the forest types during the deposition of the Middle Siwalik sediments.

Sapindaceae, Malvaceae, Verbanaceae and Vitaceae. The most diverse families in the Middle Siwalik assemblage are Fabaceae, Dipterocarpaceae, Annonaceae and Malvaceae followed by Sapindaceae, Apocynaceae, Flacourtiaceae, Moraceae, Burseraceae, Ebenaceae, Euphorbiaceae, Lauraceae, Anacardiaceae, Bombacaceae, Calophyllaceae, Clusiaceae, Compositae, Dilleniaceae, Lythraceae, Marantaceae, Oleaceae, Poaceae, Rhamnaceae, Rubiaceae, Rutaceae, Sabiaceae, Tiliaceae, Verbenaceae and Vitaceae (Figs 4c, 6). The floristic assemblage suggests that 49 % of taxa today belong to evergreen forests, whereas 24 % of taxa are affiliated with moist deciduous forests, and 27 % of taxa are evergreen to moist deciduous (Fig. 4d) (Champion & Seth, 1968).

3.b. Temperature and rainfall reconstruction of the Lower and Middle Siwalik succession of Darjeeling

In the Lower Siwalik, 25 NLR taxa have been used for the climate reconstruction (Fig. 7) and a list of all the taxa, their NLRs and numerical identifiers used are provided in Table 2.

The reconstructed temperatures for the Lower Siwalik flora are: 27.2 ± 0.3 °C for the mean annual temperature, 28.2 ± 0.1 °C for the warm month temperature and 25.6 ± 0.3 °C for the cold month temperature (Fig. 8a). The reconstructed precipitations are: 2269.5 ± 58.5 mm for the mean annual precipitation, 367 ± 4 mm for the mean precipitation during the wettest months, 31 ± 12 mm for the mean precipitation during the driest months

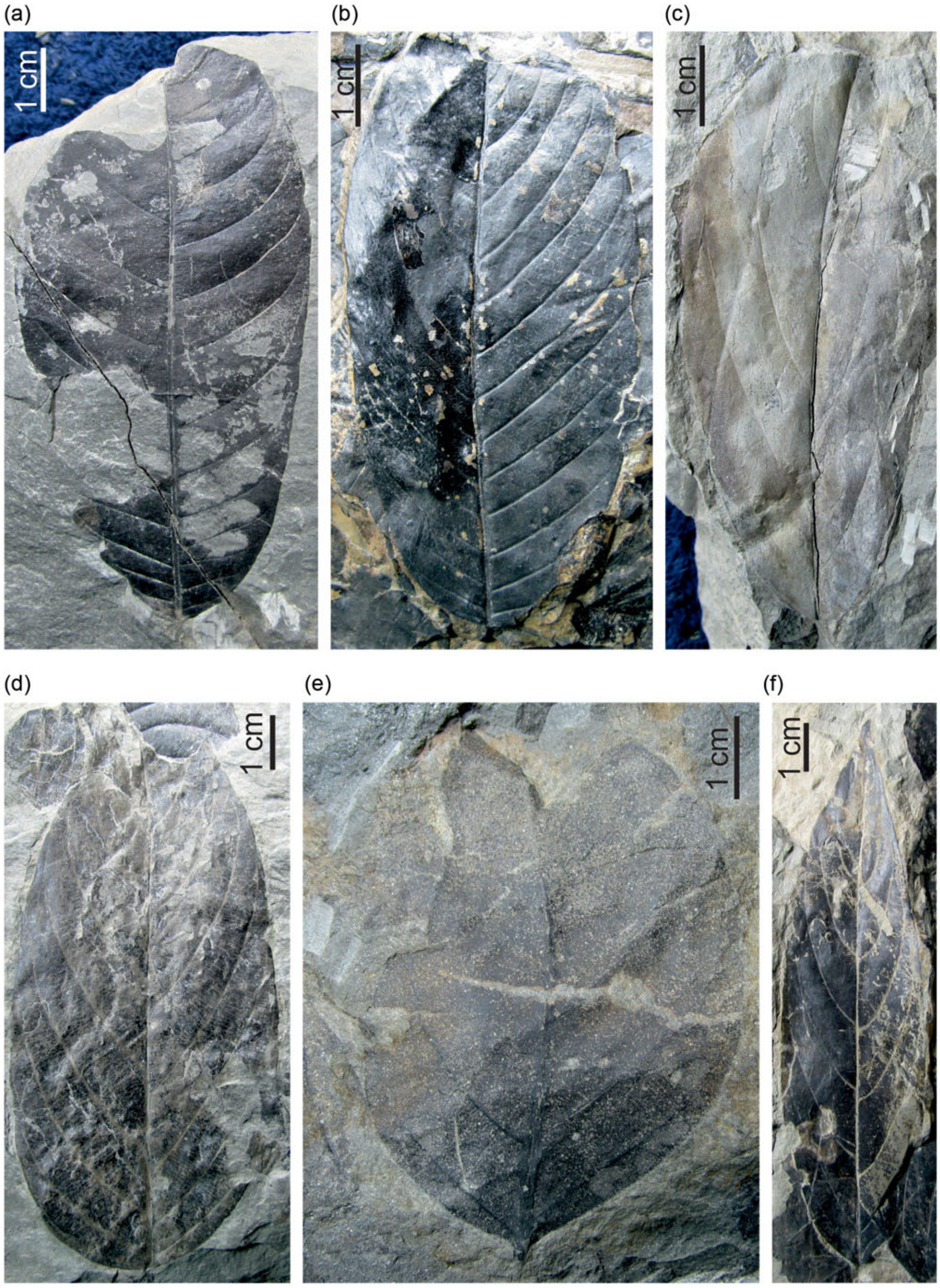

Fig. 5. (Colour online) Fossil leaf assemblage from the Lower Siwalik of Darjeeling. (a) *Combretum sahnii* Antal & Awasthi. (b) *Polyalthia palaeosimiarum* Awasthi & Prasad. (c) *Hydnocarpus palaeokurzii* Antal & Awasthi. (d) *Casearia pretomentosa* Antal & Awasthi. (e) *Pongamia siwalika* Antal & Awasthi. (f) *Nothopegia eutravancorica* Antal & Awasthi (all scale bars = 1 cm).

and 174 ± 47 mm for the mean precipitation during the warmest months (Fig. 8b). The results of the reconstruction are given in Table 3. As nearly 100 % of the NLR taxa coexist in the resulting coexistence intervals, the results are considered highly reliable (Fig. 7).

In the Middle Siwalik, 38 NLR taxa have been used for the climate reconstruction (Fig. 9) and a list of all the fossils, their NLRs and numerical identifiers are provided in Table 2. The reconstructed temperatures of the Middle Siwalik flora are: 25.5 ± 1.6 °C for the mean annual temperature, 27.6 ± 0.5 °C for the warm month temperature and 22.2 ± 2.8 °C for the cold month temperature (Fig. 8a). The precipitation reconstruction indicates 1652 ± 275 mm for the mean annual precipitation, 260.5 ± 35.5 mm for the mean precipitation during the wettest months, 38 ± 31 mm for the mean precipitation during the driest months and 152.5 ± 24.5 mm for the mean precipitation during the warmest months (Fig. 8b; Table 3). Climatic ranges of all the taxa included as NLRs overlap in the coexistence intervals (Fig. 9), again suggesting a robust result for the Middle Siwalik climate.

4. Discussion

4.a. Changing patterns in temperature and rainfall during the Lower and Middle Siwalik succession of the eastern Himalaya

The reconstructed temperature data suggest that the mean annual temperature and cold month temperature were lower by 1.7 °C and 3.4 °C, respectively, in the Middle Siwalik than in the Lower Siwalik as far as the means of their coexistence intervals are concerned,

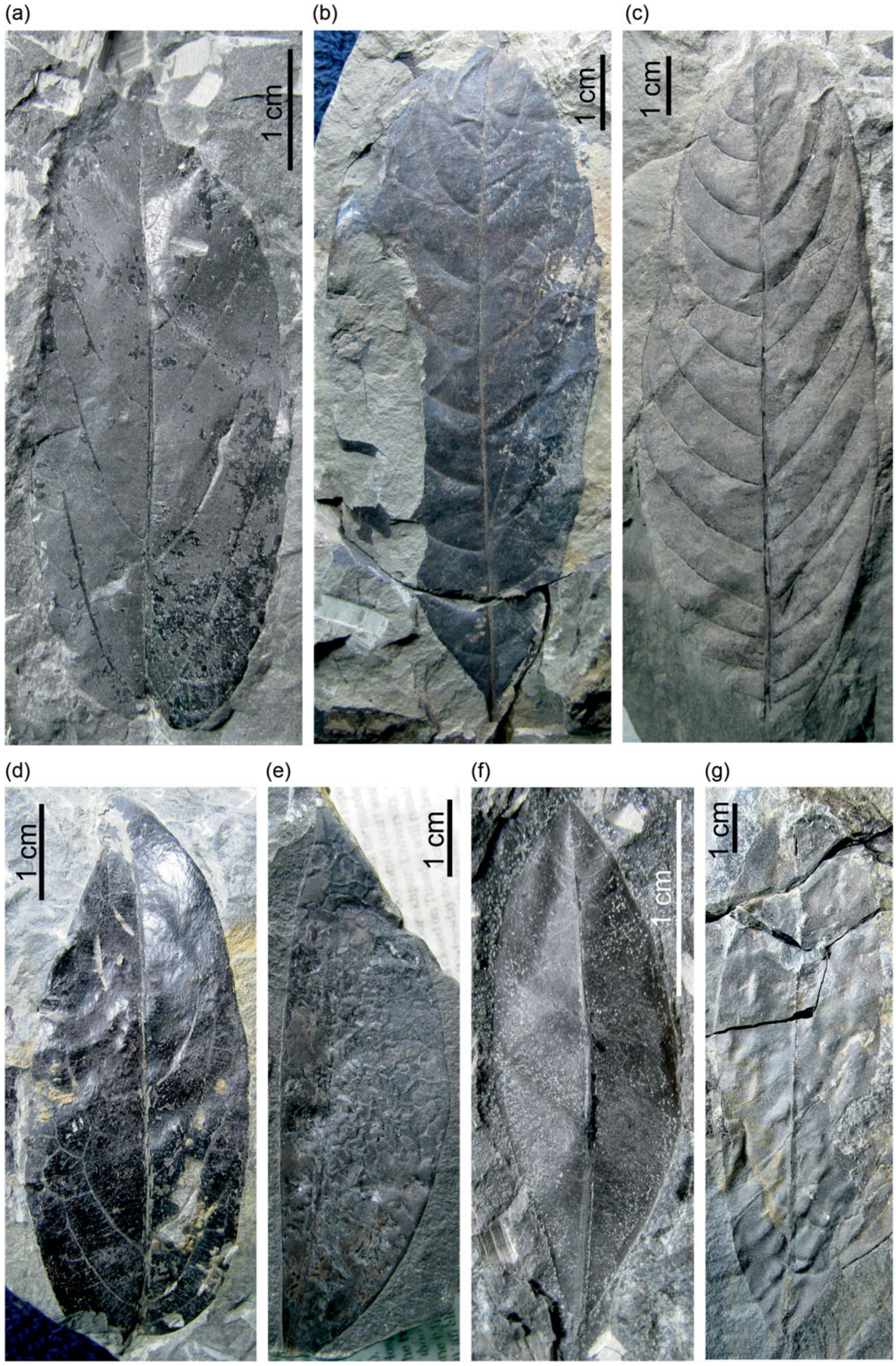

Fig. 6. (Colour online) Fossil leaf assemblage from the Middle Siwalik of Darjeeling. (a) *Grewia ghishia* Antal & Awasthi. (b) *Vitis siwalicus* Prasad *et al*. (c) *Lagerstroemia patelii* Lakhanpal & Guleria. (d) *Hopea siwalika* Antal & Awasthi. (e) *Cynometra tertiara* Antal & Awasthi. (f) *Alsodeia palaeozeylanicum* Antal & Awasthi. (g) *Calophyllum suraikholaensis* Awasthi & Prasad (all scale bars = 1 cm).

while the warm month temperature was nearly the same (Fig. 8a; Table 3). The overall reconstructed temperature data indicate that a decrease in the mean annual temperature is due to a decrease in temperature of the cooler part of the year, while the warm season remained nearly the same from the Lower to Middle Siwalik (Fig. 8a; Table 3). Our temperature reconstruction is also supported by a previous CLAMP analysis conducted by Khan *et al.* (2014) on the Lower and Middle Siwalik of Arunachal Pradesh, eastern Himalaya (Fig. 1). Considering the entire coexistence interval ranges, and confidence intervals cited for the CLAMP results, both methods show overlapping returns for all temperature estimates (Table 3). Khan *et al.* (2014) also inferred a decreasing trend in mean annual temperature and cold month temperature by 2.6 °C and 4.3 °C, while the warm month temperature remains the same (Table 3). The CLAMP methodology is entirely different from that of the CA and is based on the physics of leaf morphology and climate relationships, which is independent of taxonomic affinities (Yang *et al.* 2015).

https://doi.org/10.1017/S0016756822000243 Published online by Cambridge University Press

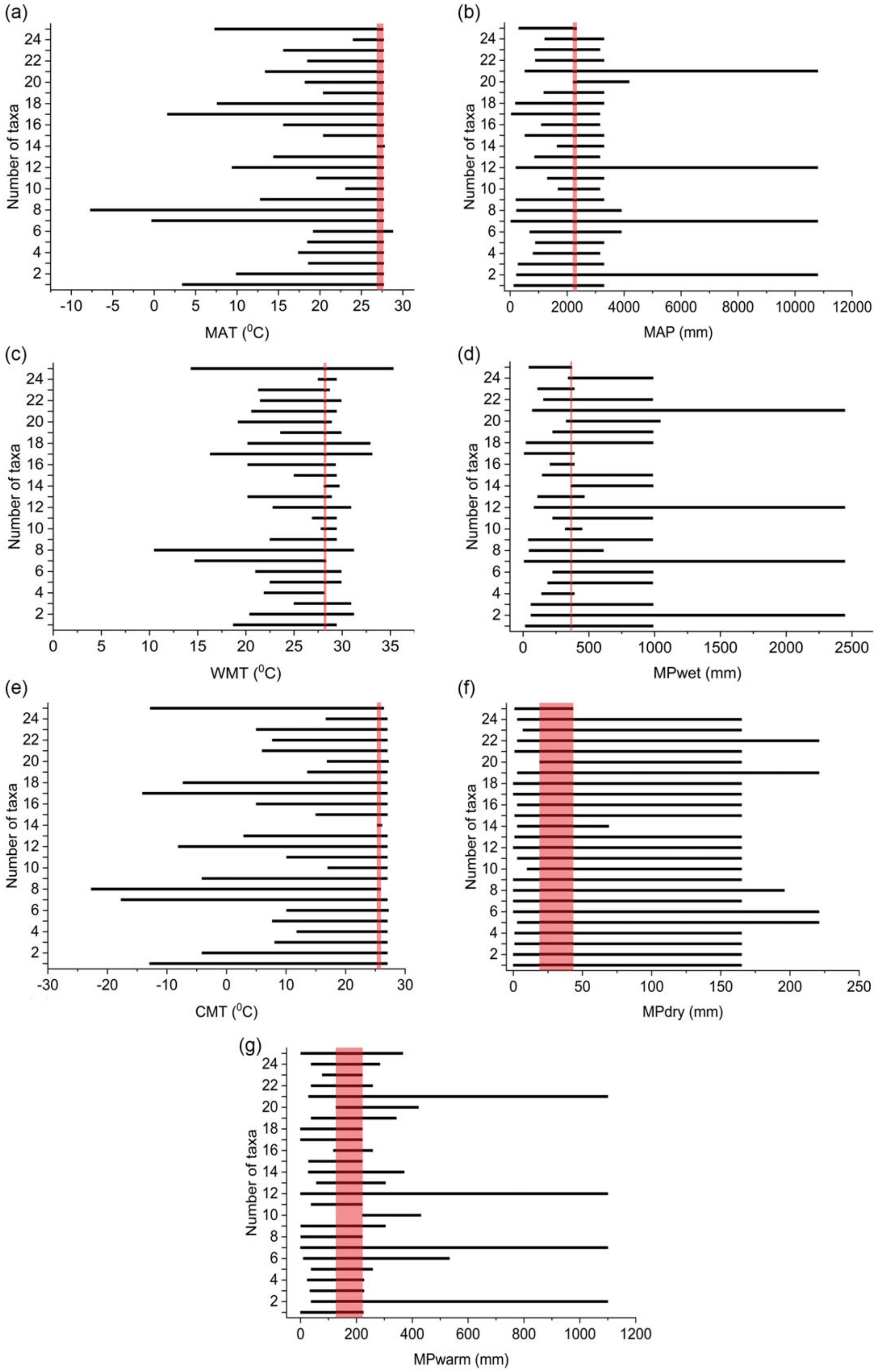

Fig. 7. (Colour online) Climatic ranges of the NLRs identified for the palaeoflora of the Lower Siwalik of Darjeeling. Red shaded areas: Coexistence Intervals (CIs). (a) Mean annual temperature (MAT). (b) Warm month mean temperature (WMT). (c) Cold month mean temperature (CMT). (d) Mean annual precipitation (MAP). (e) Mean precipitation of the wettest month (MPwet). (f) Mean precipitation of the driest month (MPdry). (g) Mean precipitation of the warmest month (MPwarm). For taxa names, see Table 2.

The rainfall reconstruction suggests a lower mean annual precipitation, mean precipitation during the wettest months and mean precipitation during the warmest months in the Middle Siwalik than in the Lower Siwalik (Table 3). This suggests that the Middle Siwalik was much drier than the Lower Siwalik. The data also imply that increased dryness in the Middle Siwalik was due to reductions in pre-monsoon (March–May/MAM) (MPwarm) and monsoon rainfall (June–September/JJAS) (MPwet) (Table 3).

https://doi.org/10.1017/S0016756822000243 Published online by Cambridge University Press

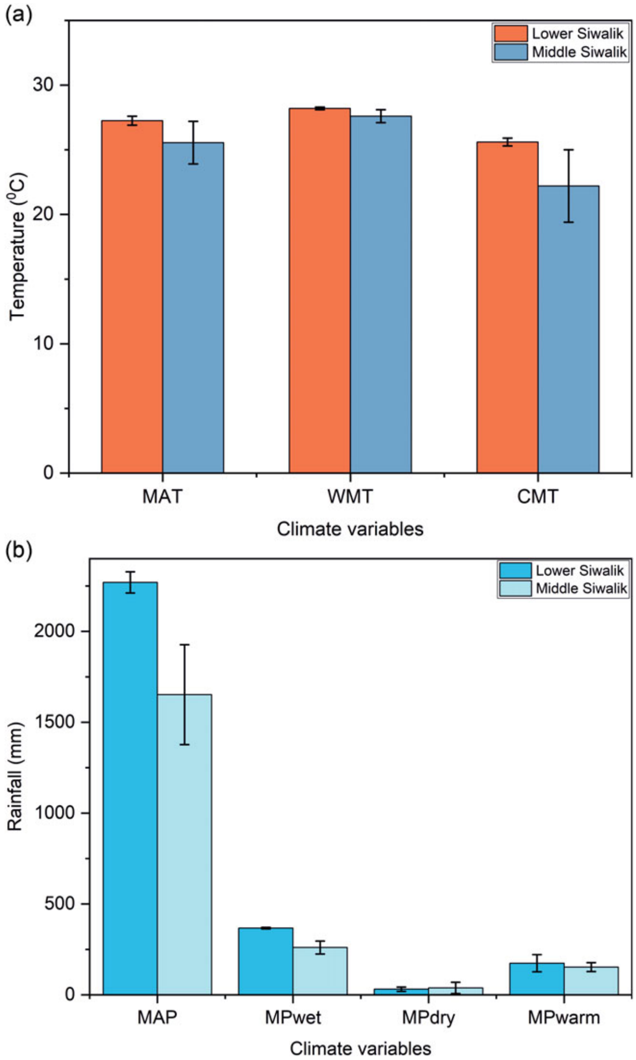

Fig. 8. (Colour online) Climate reconstruction of the Lower and Middle Siwalik. (a) Temperature reconstruction of the Lower and Middle Siwalik. (b) Bar diagram showing rainfall reconstruction of the Lower and Middle Siwalik. Abbreviations as in Figure 7.

The overall reconstructed climate data from the present and previous reconstructions (Table 3) suggest a cooling trend, particularly in the cooler (MPdry) part of the year and a decrease in pre-monsoon (MPwarm) and summer monsoon (MPwet) rainfall from the Lower to Middle Siwalik in the eastern Himalaya (Table 3).

In the western Himalaya, Sanyal *et al.* (2004), based on oxygen isotopes, suggested a high annual rainfall total at ~10.5 Ma, which subsequently weakened during 10.5–6 Ma, and again became high at 6 Ma, with a peak at 5.5 Ma. However, in the central Himalayan Siwalik, Sanyal *et al.* (2005) inferred that the monsoon became stronger after 8 Ma and attained a high level at ~6 Ma, and subsequently diminished at ~4 Ma to a level lower than that at 8 Ma. In a comparative study between the western and eastern Himalayan Siwalik, Vögeli *et al.* (2017) suggested that the modern E–W differentiation in climate was already established at ~7 Ma. Regional changes towards a more seasonal climate in the west were linked to a decrease in the winter precipitation, while the eastern part remained year-round humid, due to the proximity of an abundant moisture source from the Bay of Bengal. Srivastava *et al.* (2018) suggested that the Middle (9.5–6.8 Ma) Siwalik was drier than the Lower (~13–11 Ma) Siwalik, and this was most likely due to a decrease in rainfall during the winter season (dry season). A decrease in rainfall was also recorded from the Siwalik of Pakistan and Nepal during late Miocene time (10.5–6 Ma) (Dettman *et al.* 2001; Badgley *et al.* 2008), while increased evaporation of soil and leaf water was recorded from the upper Miocene (~9–6 Ma) of Pakistan (Nelson, 2005; Badgley *et al.* 2008). Hydrogen isotope data from the Bengal Fan show variability from 10.2 to 7.4 Ma and an increasing trend after 7.4 Ma, which suggests drying (Polissar *et al.* 2021).

The cooling in temperature and weakening of the Asian summer monsoon during the Neogene period have also been reported from other terrestrial and marine archives. Sanyal *et al.* (2004), on the basis of an oxygen isotopic study from the Siwalik of the western Himalaya, inferred that the ISM strength was higher in late Miocene time than in Pliocene time. The palynological evidence from the Surai Khola section of Nepal indicates a cooling from late Miocene to Pliocene times (Hoorn *et al.* 2000).

Neogene chemical weathering data from ODP site 718 (Bengal Fan) and Indus Marine A-1 well (Arabian Sea), along with sedimentation rates from the Indus fan, indicate an overall wetter climate in middle Miocene time than in late Miocene–Pliocene times (Clift *et al.* 2008) (Fig. 1). Moreover, recent data of increasing haematite/goethite ratios from International Ocean Discovery Program Site U1456 indicate an overall long-term drying after ~7.7 Ma (Clift *et al.* 2020) (Fig. 1). Studies based on inorganic and organic proxies derived from marine archives from the Arabian Sea, Bay of Bengal and South China Sea have inferred that the decrease in temperature and overall rainfall during late Miocene–Pliocene times might be linked with the Northern Hemisphere glaciation/cooling (Wei *et al.* 2006; Miao *et al.* 2017; Clift *et al.* 2020). All the aforesaid data either derived from continental sediments or marine sediments suggest a drying (mean annual) trend during the Neogene period.

However, recent climate modelling suggests the late Miocene to Pliocene as being a time of 'supermonsoon' and high annual rainfall total, based on overall rainfall modelled for East Asia (Farnsworth *et al.* 2019). In the future, more quantitative terrestrial palaeoclimate data are required from different regions of south Asia to better understand the linkages of a decrease in temperature and Asian monsoon dynamics during the Neogene period.

4.b. Climate and vegetation changes during Lower and Middle Siwalik time in the Himalaya

The vegetation reconstructions suggest that the Middle Siwalik (Fig. 4c) flora was more diverse than the Lower Siwalik (Fig. 4a), but many families were common to both. However, families such as Combretaceae, Meliaceae and Myrtaceae were exclusive to the Lower Siwalik (Fig. 4a), while Apocynaceae, Asteraceae, Bombacaceae, Burseraceae, Calophyllaceae, Clusiaceae, Dilleniaceae, Ebenaceae, Lauraceae, Lythraceae, Marantaceae, Oleaceae, Poaceae, Rutaceae, Sabiaceae, Verbenaceae and Vitaceae were present only in the Middle Siwalik (Fig. 4c). In the Lower Siwalik, the Flacourtiaceae family was the most dominant and was followed by members of the Fabaceae, Anacardiaceae, Annonaceae and Dipterocarpaceae. The Fabaceae family was the most dominant in the Middle Siwalik and was followed by Dipterocarpaceae, Annonaceae, Malvaceae and Sapindaceae (Fig. 4a, c).

In the Lower Siwalik, evergreen taxa dominated over those typical of moist deciduous vegetation (Fig. 4b), while in the Middle

https://doi.org/10.1017/S0016756822000243 Published online by Cambridge University Press

Table 3. Quantitative climate reconstruction of the Lower and Middle Siwalik using the Coexistence Approach (CA) (present study) and Climate Leaf Analysis Multivariate Program (CLAMP) (previous study)

Climate variables	CA of Lower Siwalik (Middle Miocene) (Darjeeling) (Present study)	CA of Middle Siwalik (Late Miocene–Pliocene) (Darjeeling) (Present study)	CLAMP of Lower Siwalik (13–10.5 Ma; Chirouze *et al.* 2012) (Arunachal Pradesh) (Khan *et al.* 2014)	CLAMP of Middle Siwalik (10.5–2.6 Ma; Chirouze *et al.* 2012) (Arunachal Pradesh) (Khan *et al.* 2014)
Mean annual temperature (°C)	27.25 ± 0.35	25.55 ± 1.65	25.3 ± 2.8	23.6 ± 2.8
Warm month mean temperature (°C)	28.2 ± 0.1	27.6 ± 0.5	27.9 ± 3.3	28.1 ± 3.3
Cold month mean temperature (°C)	25.6 ± 0.3	22.2 ± 2.8	21.3 ± 4	16.9 ± 4
Mean annual precipitation (mm)	2269.5 ± 58.5	1652 ± 275	1741.3 ± 916.2	1981.2 ± 916.2
Precipitation during the wettest months (mm)	367 ± 4	260.5 ± 35.5	–	–
Precipitation during the driest months (mm)	31 ± 12	38 ± 31	–	–
Precipitation during the warmest months (mm)	174 ± 47	152.5 ± 24.5	–	–
Precipitation during 3 wettest months (mm)	–	–	961.5 ± 528	994.1 ± 528
Precipitation during 3 driest months (mm)	–	–	73.4 ± 115	137.8 ± 115

Siwalik evergreen taxa decreased significantly and those classed as moist deciduous increased (Fig. 4d). The forest types of the Siwalik overall suggest that the evergreen taxa decreased significantly, while moist deciduous and evergreen to moist deciduous taxa increased from the Lower to Middle Siwalik (Fig. 4b, d). This change in the forest type coincides with the longer dry season (Champion & Seth, 1968). Overall, the dominance of moist deciduous forest in the Middle Siwalik in comparison to the Lower Siwalik suggests an increase in seasonal aridity.

C_4 plants are physiologically more efficient than C_3 plants and can survive under more extreme conditions such as drought, high temperatures and low CO_2 concentration. This allows them to broaden their ecological niches (Lundgren *et al.* 2016) and survive in a variety of habitats from low to high latitudes, from desert to submerged conditions, open grassland to forest understorey, and from nutrient depleted to fertile soils (Christin & Osborne, 2014). Molecular phylogenetic studies reveal that the C_4 plants evolved between 33 and 25 Ma (Gaut & Doebley, 1997; Bouchenak-Khelladi *et al.* 2009) and were most likely favoured by the lowering of atmospheric CO_2 concentration during Oligocene–early Miocene times (Tipple & Pagani, 2007). The available isotopic data indicate that the expansion of C_4 plants was not synchronous either globally (Quade *et al.* 1989, 1994; Cerling, 1992; Cerling & Quade, 1993; Cerling *et al.* 1993; Kingston *et al.* 1994; Latorre *et al.* 1997; Fox & Koch, 2003, 2004; Feakins *et al.* 2005) or regionally (Sanyal *et al.* 2010).

A large number of studies have been conducted in the western and central Himalayan Siwalik to understand the vegetation shift and expansion of C_4 plants (Quade *et al.* 1989, 1995; Tanaka, 1997; Hoorn *et al.* 2000; Sanyal *et al.* 2004, 2005, 2010; Singh *et al.* 2011; Srivastava *et al.* 2018; Karp *et al.* 2018, 2021; Tauxe & Feakins, 2020); however, few studies have been done in the eastern Himalayan Siwalik (Vögeli *et al.* 2017). The isotopic data available from the western Himalayan Siwalik indicate that C_4 plants expanded during late Miocene time (Singh *et al.* 2011 and references therein), and an increase in the dryness was inferred as the most plausible cause of their expansion (Quade *et al.* 1989, 1995; Tanaka, 1997; Hoorn *et al.* 2000; Sanyal *et al.* 2004, 2005; Srivastava *et al.* 2018). Sanyal *et al.* (2010), based on the isotopic data, suggested that the timing and nature of enrichment in the carbon isotope ratio varied from one section to another, implying that the expansion of C_4 plants in different zones of the Indian Siwaliks did not take place at the same time. They further suggested that changing monsoon intensity was not the sole cause for C_4 plant expansion in this region because monsoon intensity and C_4 plant expansion do not show a one to one correlation. Moreover, recent studies based on isotopic (oxygen and carbon) data derived from leaf wax and bivalves archived in marine (Arabian Sea and Indus River Basin) and continental (western and central Himalayan Siwalik) sediments indicate that the increase in aridity paved the way for the expansion of C_4 plants over C_3 plants (Dettman *et al.* 2001; Huang *et al.* 2007; Suzuki *et al.* 2020).

Palaeoclimatic data from the Siwalik succession of the western and central Himalaya suggest that the expansion of C_4 plants is linked to a weakening of winter rainfall brought by the WDs (Vögeli *et al.* 2017; Srivastava *et al.* 2018). The WDs are the atmospheric disturbances which bring rainfall particularly to northern India during the winter season. They originate mainly in the Mediterranean or West Atlantic region. In the Himalayan region, the WDs intensify owing to high orography and are the main source of snowfall over the region (Dimri & Chevuturi, 2016). Sometimes WDs bring heavy rainfall and heavy snowfall over the northwestern Himalaya during the winter season (Dimri & Mohanty, 1999; Dimri, 2006). In northern India, the WDs have an impact in delaying or advancing the ISM (Das *et al.* 2002).

https://doi.org/10.1017/S0016756822000243 Published online by Cambridge University Press

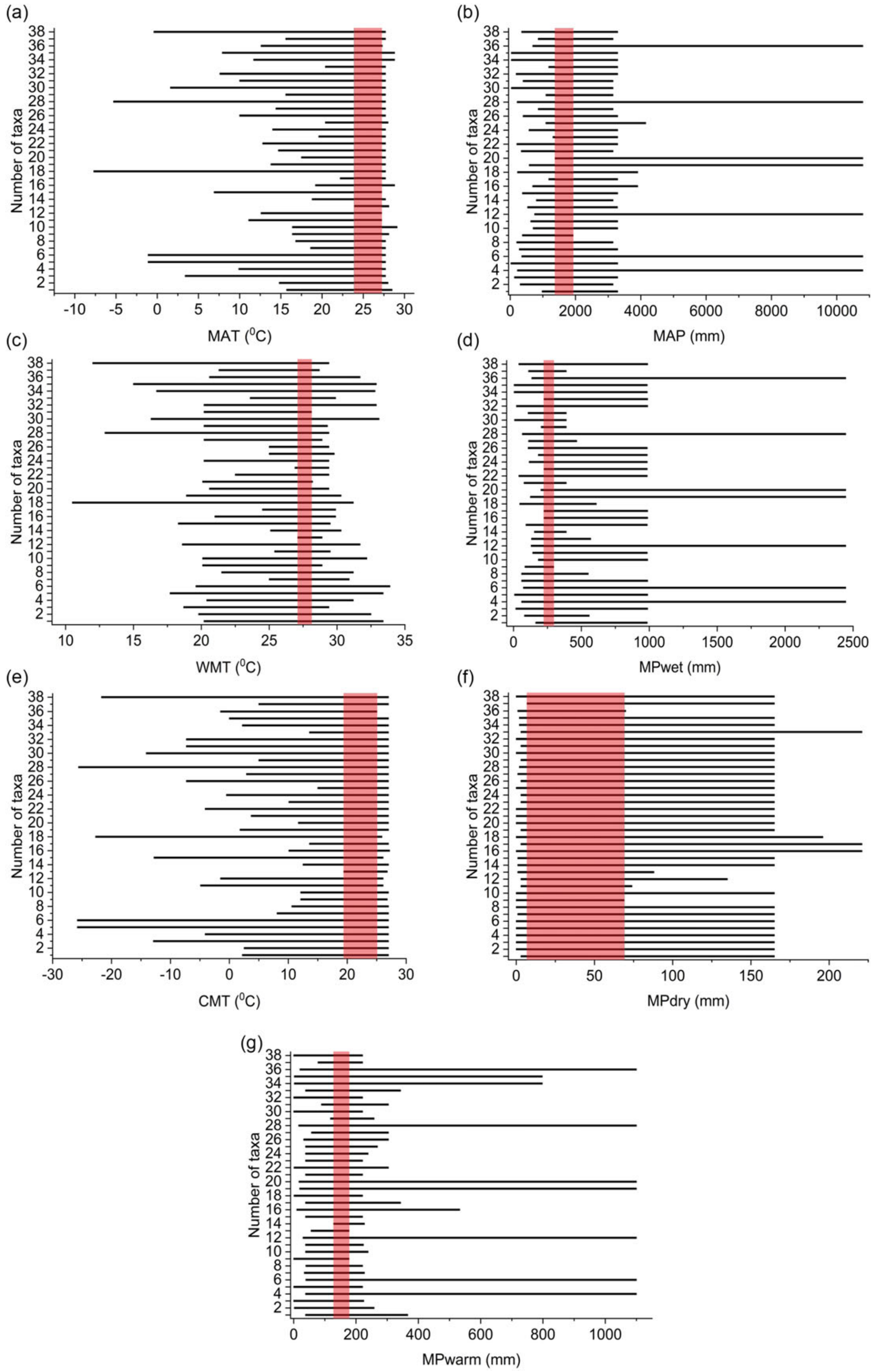

Fig. 9. (Colour online) Climatic ranges of the NLRs identified for the palaeoflora of the Middle Siwalik of Darjeeling. Red shaded areas: Coexistence Intervals (CIs). (a) Mean annual temperature (MAT). (b) Warm month mean temperature (WMT). (c) Cold month mean temperature (CMT). (d) Mean annual precipitation (MAP). (e) Mean precipitation of the wettest month (MPwet). (f) Mean precipitation of the driest month (MPdry). (g) Mean precipitation of the warmest month (MPwarm). For taxa names, see Table 2.

Beyond that, Wu *et al.* (2014) and Srivastava *et al.* (2018) have also pointed out the role of higher temperatures, particularly in the cooler part of the year, in the expansion of C_4 plants during the Middle Siwalik.

In contrast to the western and central Himalayan Siwalik, few studies are available for the eastern Himalaya to understand the C_3–C_4 vegetation change. Isotopic data from the Kameng section of the Arunachal Pradesh Siwalik suggested a persistent C_3 vegetation since 13 Ma, and this is most likely explained by the absence of seasonal climate and lack of aridity, owing to the abundant moisture supply from the Bay of Bengal (Vögeli *et al.* 2017). For the Darjeeling Siwalik no study has been done so far to understand possible C_3 and C_4 vegetation shifts during the Neogene period. However, our quantitatively reconstructed climate and vegetation data are important in understanding the dominance of seasonal forest in the Middle Siwalik (late Miocene–Pliocene) in comparison to the Lower Siwalik (middle Miocene). This expansion of seasonal forest can be related to the decrease in rainfall in the pre-monsoon (MPwarm) and monsoon seasons (MPwet) (Table 3). C_4 plants preferentially grow in seasonal forests, compared to forests that have no seasonal climate (Srivastava *et al.* 2018).

Recently, Ghosh *et al.* (2018, 2021) suggested that changes in C_3/C_4 vegetation may also depend on the substrate (sand/clay). They explained that areas of fine-grained (silt and clay) overbank sediments, far from the active channels, have a pore water deficiency and favour the growth of C_4 plants. A comparative study of the sedimentary structures among different Siwalik regions indicates that the abundance of fine-grained (silt and clay) overbank sediments is higher in the western Siwalik than the central and eastern Siwalik. The strong correlation between $\delta^{13}C$ values and abundance of fine-grained (silt and clay) overbank sediments across different Siwalik regions suggests a significant influence of substrate on the abundance of C_4 plants (Ghosh *et al.* 2018, 2021). Therefore, substrate level control in limiting the growth of C_4 vegetation since 13 Ma in NE India cannot be ignored. Moreover, the marine influence in the Himalayan Foreland Basin of NE India might also have imposed some restriction on the growth of C_4 vegetation, but this needs further investigation.

Overall, the aforesaid discussion indicates that more studies are required, particularly on the northeastern part of India, to understand the vegetation–climate relationship.

5. Conclusions

The climate of the Lower (middle Miocene) and Middle (late Miocene–Pliocene) Siwalik succession of Darjeeling (eastern Himalaya) was reconstructed using the Coexistence Approach. The reconstructed mean annual temperature and cold month temperature show a decreasing trend, while the warm month temperature remained the same from the Lower to Middle Siwalik. The CA result suggests that pre-monsoon (MPwarm) and summer monsoon rainfall (MPwet) decreased significantly from the Lower to Middle Siwalik, while winter rainfall (MPdry) remained nearly the same. The floristic assemblages suggest a vegetation shift from the dominance of evergreen taxa in the Lower Siwalik to more deciduous taxa during the Middle Siwalik. The data also suggest that the Middle Siwalik flora was more diverse than that of the Lower Siwalik.

Supplementary material. To view supplementary material for this article, please visit https://doi.org/10.1017/S0016756822000243

Acknowledgements. GS, HB and RCM are thankful to the director of the Birbal Sahni Institute of Palaeosciences, Lucknow for providing necessary facilities and encouragement during the research work. The present work was supported by SERB, New Delhi funded project no. CRG/2019/002461 and Chinese Academy of Sciences President's International Fellowship Initiative (no. 2018VMC0005) awarded to GS. The present work is a contribution to the NECLIME (Neogene Climate Evolution of Eurasia). The authors are thankful to Robert A. Spicer and two anonymous reviewers for their constructive suggestions to improve the manuscript.

Conflicts of interest. None.

References

Acharyya SK (1994) The Cenozoic foreland basin and tectonics of the Eastern Sub-Himalaya: problem and prospects. *Himalayan Geology* **15**, 3–21.

Acharyya SK (2007) Evolution of the Himalayan Paleogene foreland basin, influence of its litho-packet on the formation of thrust-related domes and windows in the Eastern Himalayas – a review. *Journal of Asian Earth Sciences* **31**, 1–17.

Acharyya SK, Dutta AK and Sastry MVA (1979) Siwalik stratigraphy and its bearing on the Main Boundary Fault. *Geological Survey of India Miscellaneous Publication* **41**, 67–79.

Acosta RP and Huber M (2020) Competing topographic mechanisms for the summer Indo-Asian Monsoon. *Geophysical Research Letters* **47**, e2019GL085112. doi: 10.1029/2019GL085112.

Antal JS and Awasthi N (1993) Fossil flora from the Himalayan foot-hills of Darjeeling District, West Bengal and its palaeoecological and phytogeographical significance. *Palaeobotanist* **42**, 14–60.

Antal JS and Prasad M (1995) Fossil leaf of *Clinogyne* Salisb. from the Siwalik sediments of Darjeeling District, West Bengal. *Geophytology* **24**, 241–3.

Antal JS and Prasad M (1996a) Some more leaf-impressions from the Himalayan foot-hills of Darjeeling District, West Bengal, India. *Palaeobotanist* **43**, 1–9.

Antal JS and Prasad M (1996b) Dipterocarpaceous fossil leaves from Ghish River section in Himalayan foot hills near Oodlabari, Darjeeling District, West Bengal. *Palaeobotanist* **43**, 73–7.

Antal JS and Prasad M (1996c) Leaf-impressions of *Polyalthia* Bl. in the Siwalik sediments of Darjeeling District, West Bengal. *Geophytology* **26**, 125–7.

Antal JS and Prasad M (1997) Angiospermous fossil leaves from the Siwalik sediments (Middle-Miocene) of Darjeeling District, West Bengal. *Palaeobotanist* **46**, 95–104.

Antal JS and Prasad M (1998) Morphotaxonomic study of some more fossil leaves from the Lower Siwalik sediments of West Bengal, India. *Palaeobotanist* **47**, 86–98.

Antal JS, Prasad M and Khare EG (1996) Fossil woods from the Siwalik sediments of Darjeeling District, West Bengal, India. *Palaeobotanist* **43**, 98–105.

Badgley C, Barry JC, Morgan ME, Nelson SV, Behrensmeyer AK, Cerling TE and Pilbeam D (2008) Ecological changes in Miocene mammalian record show impact of prolonged climatic forcing. *Proceedings of the National Academy of Sciences of the United States of America* **105**, 12145–9.

Bhatia H, Khan MA, Srivastava G, Hazra T, Spicer RA, Hazra M, Mehrotra RC, Spicer TEV, Bera S and Roy K (2021a) Late Cretaceous–Paleogene Indian monsoon climate vis-à-vis movement of the Indian plate, and the birth of the South Asian Monsoon. *Gondwana Research* **93**, 89–100.

Bhatia H, Srivastava G, Spicer RA, Farnsworth A, Spicer TEV, Mehrotra RC, Paudayal KN and Valdes P (2021b) Leaf physiognomy records the Miocene intensification of the south Asia monsoon. *Global and Planetary Change* **196**, 103365. doi: 10.1016/j.gloplacha.2020.103365.

Bondarenko OV, Blochina NI and Utescher T (2013) Quantification of Calabrian climate in southern Primory'e, Far East of Russia — an integrative case study using multiple proxies. *Palaeogeography, Palaeoclimatology, Palaeoecology* **386**, 445–58.

Boos WR and Kuang Z (2010) Dominant control of the South Asian monsoon by orographic insulation versus plateau heating. *Nature* **463**, 218–22.

Boos WR and Kuang Z (2013) Sensitivity of the South Asian monsoon to elevated and non-elevated heating. *Scientific Reports* **3**, 1192. doi: 10.1038/srep01192.

https://doi.org/10.1017/S0016756822000243 Published online by Cambridge University Press

Bouchenak-Khelladi Y, Verboom GA, Hodkinson TR, Salamin N, Francois O, Chonghaile GN and Savolainen V (2009) The origins and diversification of C_4 grasses and savanna adapted ungulates. *Global Change Biology* **15**, 2397–417.

Cerling TE (1992) Development of grasslands and savannas in East Africa during the Neogene. *Palaeogeography, Palaeoclimatology, Palaeoecology* **97**, 241–7.

Cerling TE and Quade J (1993) Stable carbon and oxygen isotopes in soil carbonates. In *Climate Change in Continental Isotopic Records* (eds PK Swart, KC Lohmann, J McKenzie and S Savin), pp. 217–32. American Geophysical Union, Monograph vol. 78. Washington, DC, USA.

Cerling TE, Wang Y and Quade J (1993) Expansion of C4 ecosystems as an indicator of global ecological change in the late Miocene. *Nature* **361**, 344–5.

Chakraborty T, Taral S, More S and Bera S (2020) Cenozoic Himalayan Foreland Basin: an overview and regional perspective of the evolving sedimentary succession. In *Geodynamics of the Indian Plate* (eds N Gupta and SK Tandon), pp. 395–437. Cham: Springer International Publishing.

Chaloner WG and Creber GT (1990) Do fossil plants give a climatic signal? *Journal of the Geological Society, London* **147**, 343–50.

Champion HG and Seth SK (1968) *A Revised Survey of Forest Types of India*. New Delhi: Government of India Press.

Chirouze F, Dupont-Nivet G, Huyghe P, van der Beek P, Chakraborti T, Bernet M and Erens V (2012) Magnetostratigraphy of the Neogene Siwalik Group in the far eastern Himalaya: Kameng section, Arunachal Pradesh, India. *Journal of Asian Earth Sciences* **44**, 117–35.

Christin P-A and Osborne CP (2014) The evolutionary ecology of C_4 plants. *New Phytologist* **204**, 765–81.

Clift PD, Hodges KV, Heslop D, Hannigan R, Long HV and Calves G (2008) Correlation of Himalayan exhumation rates and Asian monsoon intensity. *Nature Geoscience* **1**, 875–80.

Clift PD, Kulhanek DK, Zhou P, Bowen MG, Vincent SM, Lyle M and Hahn A (2020) Chemical weathering and erosion responses to changing monsoon climate in the Late Miocene of Southwest Asia. *Geological Magazine* **157**, 939–55.

India Meteorological Department (1931–1960) *Climatological Tables of Observatories in India*. Nasik: Government of India Press.

Coutand I, Barrier L, Govin G, Grujic D, Hoorn C, Dupont-Nivet G and Najman Y (2016) Late Miocene–Pleistocene evolution of India–Eurasia convergence partitioning between the Bhutan Himalaya and the Shillong Plateau: new evidences from foreland basin deposits along the Dungsam Chu section, eastern Bhutan. *Tectonics* **35**, 2963–94.

Das MR, Mukhopadhyay RK, Dandekar MM and Kshirsagar SR (2002) Pre-monsoon western disturbances in relation to monsoon rainfall, its advancement over NW India and their trends. *Current Science* **82**, 1320–1.

DeCelles PG, Gehrels GE, Quade J and Ojha TP (1998) Eocene-early Miocene foreland basin development and the history of Himalayan thrusting, western and central Nepal. *Tectonics* **17**, 741–65.

Dettman DL, Kohn MJ, Quade J, Ryerson FJ, Ojha TP and Hamidullah S (2001) Seasonal stable isotope evidence for a strong Asian monsoon throughout the past 10.7 m.y. *Geology* **29**, 31–4.

Dimri AP (2006) Surface and upper air fields during extreme winter precipitation over the Western Himalayas. *Pure and Applied Geophysics* **163**, 1679–98.

Dimri AP and Chevuturi A (2016) *Western Disturbances: An Indian Meteorological Perspective*. Cham: Springer International Publishing.

Dimri AP and Mohanty UC (1999) Snowfall statistics of some SASE field stations in J&K. *Defence Science Journal* **49**, 437–45.

Ding L, Spicer RA, Yang J, Xu Q, Cai F, Li S, Lai Q, Wang H, Spicer TEV, Yue Y, Shukla A, Srivastava G, Khan MA, Bera S and Mehrotra R (2017) Quantifying the rise of the Himalaya orogen and implications for the South Asian monsoon. *Geology* **45**, 215–8.

Farnsworth A, Lunt DJ, Robinson SA, Valdes PJ, Roberts WHG, Clift PD, Markwick P, Su T, Wrobel N, Bragg F, Kelland S-J and Pancost RD (2019) Past East Asia monsoon evolution controlled by paleogeography, not CO_2. *Science Advances* **5**, eaas1697. doi: 10.1126/sciadv.aax1697.

Feakins SJ, deMenocal PB and Eglinton TIB (2005) Biomarker records of late Neogene changes in northeast African vegetation. *Geology* **33**, 977–80.

Fox DL and Koch PL (2003) Tertiary history of C_4 biomass in the Great Plains, USA. *Geology* **31**, 809–12.

Fox DL and Koch PL (2004) Carbon and oxygen isotopic variability in Neogene palaeosol carbonates: constraints on the evolution of the C_4-grasslands of the Great Plains, USA. *Palaeogeography, Palaeoclimatology, Palaeoecology* **207**, 305–29.

Ganguly S and Rao DP (1970) Stratigraphy and structure of the Tertiary foothills of Eastern Himalaya. Darjeeling District. *Quarterly Journal of the Geological, Mining and Metallurgical Society of India* **42**, 185–95.

Gaut BS and Doebley JF (1997) DNA sequence evidence for the segmental allotriploid origin of maize. *Proceedings of National Academy of Sciences of the United States of America* **94**, 6809–14.

Ghosh S, Bera ML, Roy B and Sanyal P (2021) Revisiting the diachronous transition of C_3 to C_4 plants in the Himalayan foreland and other parts of the globe: a sedimentological perspective. *Sedimentology* **68**, 2473–99. doi: 10.1111/sed.12865.

Ghosh S, Sanyal P, Sangode SJ and Nanda AC (2018) Substrate control of C_4 plant abundance in the Himalayan foreland: a study based on inter-basinal records from Plio-Pleistocene Siwalik Group. *Palaeogeography, Palaeoclimatology, Palaeoecology* **511**, 341–51.

Givnish TJ (1984) Leaf and canopy adaptations in tropical forest. In *Physiological Ecology of Plants of the Wet Tropics* (eds E Medina, HA Mooney and C Vázquez-Yáñez), pp. 51–84. The Hague: Dr W. Junk Publishers.

Goswami BN, Krishnamurthy V and Annamalai H (1999) A broad scale circulation index for the interannual variability of the Indian summer monsoon. *Quarterly Journal of the Royal Meteorological Society* **125**, 611–33.

Hickey LJ (1977) *Stratigraphy and Paleobotany of the Golden Valley Formation (Early Tertiary) of Western North Dakota*. Geological Society of America Memoirs vol. 150, 183 pp.

Hoorn C, Ohja T and Quade J (2000) Palynological evidence for vegetation development and climate change in the Sub-Himalayan Zone (Neogene, Central Nepal). *Palaeogeography, Palaeoclimatology, Palaeoecology* **163**, 133–61.

Huang Y, Clemens SC, Liu W, Wang Y and Prell WL (2007) Large-scale hydrological change drove the late Miocene C4 plant expansion in the Himalayan foreland and Arabian Peninsula. *Geology* **35**, 531–4.

Jain AK, Banerjee DM and Kale VS (2020) *Tectonics of the Indian Subcontinent*. Cham: Springer International Publishing.

Joshi A, Tewari R, Mehrotra RC, Chakraborty PP and De A (2003) Plant remains from the Upper Siwalik sediments of West Kameng District, Arunachal Pradesh. *Journal of the Geological Society of India* **61**, 319–24.

Juenger T, Pérez-Pérez J and Mand Micol JL (2005) Quantitative trait loci mapping of floral and leaf morphology traits in *Arabidopsis thaliana*: evidence for modular genetic architecture. *Evolution and Development* **7**, 259–71.

Karp AT, Behrensmeyer AK and Freeman KH (2018) Grassland fire ecology has roots in the late Miocene. *Proceedings of the National Academy of Sciences of the United States of America* **115**, 12130–5.

Karp AT, Uno KT, Polissar PJ and Freeman KH (2021) Late Miocene C_4 grassland fire feedbacks on the Indian Subcontinent. *Paleoceanography and Palaeoclimatology* **36**, e2020PA004106. doi: 10.1029/2020PA004106.

Khan MA, Spicer RA, Bera S, Ghosh R, Yang J, Spicer TEV, Guo SX, Su T, Jacques F and Grote PJ (2014) Miocene to Pleistocene floras and climate of the eastern Himalayan Siwaliks, and new palaeoelevation estimates for the Namling–Oiyug Basin, Tibet. *Global and Planetary Change* **113**, 1–10.

Khan MA, Spicer RA, Spicer TEV and Bera S (2016) Occurrence of *Shorea* Roxburgh ex C.F. Gaertner (Dipterocarpaceae) in the Neogene Siwalik forests of eastern Himalaya and its biogeography during the Cenozoic of Southeast Asia. *Review of Palaeobotany and Palynology* **233**, 236–54.

Kingston JD, Marino BD and Hill A (1994) Isotopic evidence for Neogene hominid paleoenvironments in the Kenya Rift Valley. *Science* **264**, 955–9.

Kumar R, Ghosh SK, Mazari RK and Sangode SJ (2003a) Tectonic impact on the fluvial deposits of Plio-Pleistocene Himalayan foreland basin, India. *Sedimentary Geology* **158**, 209–34.

Kumar R, Ghosh SK and Sangode SJ (2003b) Mio-Pliocene sedimentation history in the northwestern part of the Himalayan foreland basin, India. *Current Science* **84**, 1006–13.

https://doi.org/10.1017/S0016756822000243 Published online by Cambridge University Press

Kumar R, Ghosh SK and Sangode SJ (2011) Sedimentary architecture of late Cenozoic Himalayan foreland basin fill: an overview. *Memoirs of the Geological Society of India* **78**, 245–80.

Latorre C, Quade J and McIntosh WC (1997) The expansion of C_4 grasses and global climate change in the late Miocene: stable isotope evidence from the Americas. *Earth and Planetary Science Letters* **146**, 83–96.

Liang M, Bruch A, Collinson ME, Mosbrugger V, Li C-S, Sun Q and Hilton J (2003) Testing the climatic signals from different palaeobotanical methods: an example from the middle Miocene Shanwang flora of China. *Palaeogeography, Palaeoclimatology, Palaeoecology* **198**, 279–301.

Liu XD and Yin ZY (2002) Sensitivity of East Asian monsoon climate to the uplift of the Tibetan Plateau. *Palaeogeography, Palaeoclimatology, Palaeoecology* **183**, 223–45.

Lundgren MR, Christin PA, Escobar EG, Ripley BS, Besnard G, Long CM, Hattersley PW, Ellis RP, Leegood RC and Osborne CP (2016) Evolutionary implications of C_3–C_4 intermediates in the grass *Alloteropsis semialata*. *Plant Cell and Environment* **39**, 1874–85.

MacGinitie HD (1941) *A Middle Eocene Flora From the Central Sierra Nevada*. Washington: Carnegie Institute of Washington Publication no. 534, pp. 1–94.

Mahanta R, Sarma D and Choudhury A (2013) Heavy rainfall occurrences in northeast India. *International Journal of Climatology* **33**, 1456–69.

Matin A and Mukul M (2010) Phases of deformation from cross-cutting structural relationships in external thrust sheets: insights from small-scale structures in the Ramgarh thrust sheet, Darjeeling Himalaya, West Bengal. *Current Science* **99**, 1369–77.

Miao Y, Herrmann M, Wu F, Yan X and Yang S (2012) What controlled Mid–Late Miocene long-term aridification in Central Asia? — global cooling or Tibetan Plateau uplift: a review. *Earth-Science Reviews* **112**, 155–72.

Miao Y, Warny S, Clift PD, Liu C and Gregory M (2017) Evidence of continuous Asian summer monsoon weakening as response to global cooling over the last 8 Ma. *Gondwana Research* **52**, 48–58.

Mitra S, Bera S and Banerjee M (2000) Palynofloral assemblage from Siwalik foredeep Neogene sediments of Darjeeling foothills, Eastern Himalaya. *Geophytology* **28**, 121–7.

Molnar P, Boos WR and Battisti DS (2010) Orographic controls on climate and paleoclimate of Asia: thermal and mechanical roles for the Tibetan Plateau. *Annual Review of Earth and Planetary Sciences* **38**, 77–102.

More S, Paruya DK, Taral S, Chakraborty T and Bera S (2016) Depositional environment of Mio-Pliocene Siwalik sedimentary strata from the Darjeeling Himalayan Foothills, India: a palynological approach. *PLoS One* **11**, e0150168. doi: 10.1371/journal.pone.0150168.

More S, Rit R, Khan MA, Paruya DK, Taral S, Chakraborty T and Bera S (2018) Record of leaf and pollen cf. *Sloanea* (Elaeocarpaceae) from the Middle Siwalik of Darjeeling sub-Himalaya, India and its paleobiogeographic implications. *Journal of the Geological Society of India* **91**, 301–6.

Mosbrugger V (1999) The nearest living relative method. In *Fossil Plants and Spores: Modern Techniques* (eds TP Jones and NP Rowe), pp. 261–5. Bath: Geological Society of London.

Mosbrugger V and Utescher T (1997) The coexistence approach — a method for quantitative reconstructions of Tertiary terrestrial palaeoclimate data using plant fossils. *Palaeogeography, Palaeoclimatology, Palaeoecology* **134**, 61–86.

Mosbrugger V, Utescher T and Dilcher DL (2005) Cenozoic continental climatic evolution of Central Europe. *Proceedings of the National Academy of Sciences of the United States of America* **102**, 14964–9.

Nakayama K and Ulak PD (1999) Evolution of fluvial style in the Siwalik Group in the foothills of the Nepal Himalaya. *Sedimentary Geology* **125**, 205–24.

Nelson SV (2005) Paleoseasonality inferred from equid teeth and intra-tooth isotopic variability. *Palaeogeography, Palaeoclimatology, Palaeoecology* **222**, 122–44.

Ohja TP, Butler B, Quade J and DeCelles P (2000) Magnetic polarity stratigraphy of the Neogene Siwalik Group at Khutia Khola, far western Nepal. *Geological Society of America Bulletin* **112**, 424–34.

Parthasarathy B and Dhar ON (1974) Secular variations of regional rainfall over India. *Quarterly Journal of the Royal Meteorological Society* **100**, 245–57.

Parthasarathy B, Munot AA and Kothawale DR (1995) *Monthly and Seasonal Time Series for All India Homogeneous Regions and Meteorological Subdivisions: 1871–1994*. Research Report No. RR065. Pune, India: Indian Institute of Tropical Meteorology, 113 pp.

Parthasarathy B, Rupakumar K and Kothawale DR (1992) Indian summer monsoon rainfall indices, 1871–1990. *Meteorological Magazine* **121**, 174–86.

Pigliucci M (2003) Phenotypic integration: studying the ecology and evolution of complex phenotypes. *Ecology Letters* **6**, 265–72.

Pilgrim GE (1910) Preliminary note on a revised classification of the Tertiary fresh-water deposits of India. *Records of the Geological Survey of India* **40**, 185–205.

Pilgrim GE (1913) The correlation of the Siwalik with mammal horizons of Europe. *Records of the Geological Survey of India* **43**, 264–326.

Polissar PJ, Uno KT, Phelps SR, Karp AT, Freeman KH and Pensky JL (2021) Hydrologic changes drove the late Miocene expansion of C_4 grasslands on the Northern Indian subcontinent. *Paleoceanography and Paleoclimatology* **36**, e2020PA004108. doi: 10.1029/2020PA004108.

Prasad M, Panjawani M, Kannaujia AK and Alok (2009) Siwalik fossil leaves from the Himalayan foothills of the Darjeeling District, West Bengal, India and their significance. In *Proceedings of National Seminar on Environmental Degradation and Biodiversity: Problem and Prospects, 29–30 November, 2009*, pp. 27–32.

Prasad M, Kannaujia AK, Alok and Singh SK (2015) Plant megaflora from the Siwalik (Upper Miocene) of Darjeeling District, West Bengal, India and its palaeoclimatic and phytogeographic significance. *Palaeobotanist* **64**, 13–94.

Qin F, Ferguson D, Zetter R, Wang Y, Syabrya S, Li J, Yang J and Li C-S (2011) Late Pliocene vegetation and climate of Zhangcun region, Shanxi, North China. *Global Change Biology* **17**, 1850–70.

Quade J, Cater MLJ, Ojha PT, Adam J and Harrison MT (1995) Late Miocene environmental change in Nepal and the northern Indian subcontinent: stable isotopic evidence from paleosols. *Geological Society of America Bulletin* **107**, 1381–97.

Quade J, Cerling TE and Bowman JR (1989) Development of Asian monsoon revealed by marked ecological shift during the latest Miocene in northern Pakistan. *Nature* **342**, 163–6.

Quade J, Solounias N and Cerling TE (1994) Stable isotopic evidence from palaeosol carbonates and fossil teeth in Greece for forest or woodlands over the past 11 Ma. *Palaeogeography, Palaeoclimatology, Palaeoecology* **108**, 41–53.

Ranga Rao A (1983) Geology and hydrocarbon potential of a part of Assam-Arankan basin and its adjacent region. *Petroleum Asia Journal* **4**, 127–58.

Rodriguez RE, Debernardi JM and Palatnik JF (2014) Morphogenesis of simple leaves: regulation of leaf size and shape. *WIREs Developmental Biology* **3**, 41–57.

Rowley DB (1996) Age of initiation of collision between India and Asia: a review of stratigraphic data. *Earth and Planetary Science Letters* **145**, 1–13.

Roy B, Roy S, Goyal K, Ghosh S and Sanyal P (2021) Biomarker and carbon isotopic evidence of marine incursions in the Himalayan foreland basin during its overfilled stage. *Paleoceanography and Paleoclimatology* **36**, e2020PA004083. doi: 10.1029/2020PA004083.

Rundel PW (1999) *Forest Habitats and Floristics of Indochina: Lao PDR, Cambodia and Vietnam*. Hanoi: World Wide Fund for Nature (WWF).

Sanyal P, Bhattacharya SK, Kumar R, Ghosh SK and Sangode SJ (2004) Mio-Pliocene monsoonal record from Himalayan foreland basin (Indian Siwalik) and its relation to vegetational change. *Palaeogeography, Palaeoclimatology, Palaeoecology* **205**, 23–41.

Sanyal P, Bhattacharya SK and Prasad M (2005) Chemical diagenesis of Siwalik sandstone: isotopic and mineralogical proxies from Surai Khola section, Nepal. *Palaeogeography, Palaeoclimatology, Palaeoecology* **180**, 57–74.

Sanyal P, Sarkar A, Bhattacharya SK, Kumar R, Ghosh SK and Agrawal S (2010) Intensification of monsoon, microclimate and asynchronous C_4 appearance: isotopic evidence from the Indian Siwalik sediments. *Palaeogeography, Palaeoclimatology, Palaeoecology* **296**, 165–73.

Singh S, Parkash B, Awasthi AK and Kumar S (2011) Late Miocene record of palaeo-vegetation from the Siwalik palaeosols of the Ramnagar sub-basin. *Current Science* **100**, 213–22.

Singh T and Tripathi SKM (1990) Siwalik sediments of Arunachal Himalaya: palynology, palaeoecology and palaeogeography. *Palaeobotanist* **38**, 325–32.

Sinha NK, Chatterjee BP and Satsangi PP (1982) Status of paleontological researches in the northeastern states of India. *Records of the Geological Survey of India* **112**, 66–88.
Spicer RA, Yang J, Herman AB, Kodrul T, Maslova N, Spicer TEV, Aleksandrova GN and Jin J (2016) Asian Eocene monsoons as revealed by leaf architectural signatures. *Earth and Planetary Science Letters* **449**, 61–8.
Spicer RA, Yang J, Spicer TEV and Farnsworth A (2021) Woody dicot leaf traits as a palaeoclimate proxy: 100 years of development and application. *Palaeogeography, Palaeoclimatology, Palaeoecology* **562**, 110138. doi: 10.1016/j.palaeo.2020.110138.
Srivastava G, Paudayal KN, Utescher T and Mehrotra RC (2018) Miocene vegetation shift and climate change: evidence from the Siwalik of Nepal. *Global and Planetary Change* **161**, 108–20.
Srivastava G, Tiwari RP and Mehrotra RC (2017) Quantification of rainfall during the late Miocene–early Pliocene in north east India. *Current Science* **113**, 2253–7.
Srivastava G, Trivedi A, Mehrotra RC, Paudayal KN, Limaye RB, Kumaran KPN and Yadav SK (2016) Monsoon variability over Peninsular India during Late Pleistocene: signatures of vegetation shift recorded in terrestrial archive from the corridors of Western Ghats. *Palaeogeography, Palaeoclimatology, Palaeoecology* **443**, 57–65.
Suzuki K, Yamamoto M and Seki O (2020) Late Miocene changes in C_3, C_4 and aquatic plant vegetation in the Indus River basin: evidence from leaf wax $\delta^{13}C$ from Indus Fan sediments. *Geological Magazine* **157**, 979–88.
Tanaka S (1997) Uplift of the Himalaya and climatic change at 10 Ma—evidence from records of carbon stable isotopes and fluvial sediments in the Churia Group, central Nepal. *Journal of the Geological Society of Japan* **103**, 253–64.
Tandon SK (1991) The Himalayan Foreland: focus on Siwalik Basin. In *Sedimentary Basins of India: Tectonic Context* (eds SK Tandon, CC Pant and SM Casshyap), pp. 177–201. Nainital, India: Gyanodaya Prakashan.
Taral S and Chakraborty T (2018) Deltaic coastline of the Siwalik (Neogene) foreland basin: evidences from the Gish River section, Darjeeling Himalaya. *Geological Journal* **53**, 203–29.
Taral S, Kar N and Chakraborty T (2017) Wave-generated structures in the Siwalik rocks of Tista valley, eastern Himalaya: implication for regional palaeogeography. *Current Science* **113**, 889–901.
Tauxe L and Feakins SJ (2020) A reassessment of the chronostratigraphy of late Miocene C_3–C_4 transitions. *Paleoceanography and Paleoclimatology* **35**, e2020PA003857. doi: 10.1029/2020PA003857.
Tipple BJ and Pagani M (2007) The early origins of terrestrial C_4 photosynthesis. *Annual Review of Earth Planetary Sciences* **35**, 435–61.
Tiwari RP, Mehrotra RC, Srivastava G and Shukla A (2012) The vegetation and climate of a Neogene petrified wood forest of Mizoram, India. *Journal of Asian Earth Sciences* **61**, 143–65.
Uddin A and Lundberg N (2004) Miocene sedimentation and subsidence during continent–continent collision, Bengal basin, Bangladesh. *Sedimentary Geology* **164**, 131–46.
Uhl D, Klotz S, Traiser C, Thiel C, Utescher T, Kowalski E and Dilcher DL (2007) Cenozoic paleotemperatures and leaf physiognomy — a European perspective. *Palaeogeography, Palaeoclimatology, Palaeoecology* **248**, 24–31.
Utescher T, Bondarenk OV and Mosbrugger V (2015) The Cenozoic cooling–continental signals from the Atlantic and Pacific side of Eurasia. *Earth and Planetary Science Letters* **415**, 121–33.
Utescher T, Bruch AA, Erdei B, François L, Ivanov D, Jacques FMB, Kern AK, Liu Y-SC, Mosbrugger V and Spicer RA (2014) The coexistence approach—theoretical background and practical considerations of using plant fossils for climate quantification. *Palaeogeography, Palaeoclimatology, Palaeoecology* **410**, 58–73.
Vögeli N, Najman Y, van der Beek P, Huyghe P, Wynn PM, Govin G, van der Veen I and Sachse D (2017) Lateral variations in vegetation in the Himalaya since the Miocene and implications for climate evolution. *Earth and Planetary Science Letters* **471**, 1–9.
Wang B and Fan Z (1999) Choice of south Asian summer monsoon indices. *Bulletin of the American Meteorological Society* **80**, 629–38.
Wang B, Xiang B, Li J, Webster PJ, Rajeevan MN, Liu J and Ha K-J (2015) Rethinking Indian monsoon rainfall prediction in the context of recent global warming. *Nature Communication* **6**, 7154. doi: 10.1038/ncomms8154.
Wang H, Lu H, Zhao L, Zhang H, Lei F and Wang Y (2019) Asian monsoon rainfall variation during the Pliocene forced by global temperature change. *Nature Communications* **10**, 5272. doi: 10.1038/s41467-019-13338-4.
Wang PX, Wang B, Cheng H, Fasullo J, Guo Z-T, Liu Z-Y and Kiefer T (2017) The global monsoon across time scales: mechanisms and outstanding issues. *Earth-Science Reviews* **174**, 84–121.
Webster PJ (1987) The variable and interactive monsoon. In *Monsoon* (eds JS Fein and P Stephens), pp. 268–330. New York: John Wiley.
Wei G, Li X-H, Liu Y, Shao L and Liang X (2006) Geochemical record of chemical weathering and monsoon climate change since the early Miocene in the South China Sea. *Palaeoceanography* **21**, PA4214. doi: 10.1029/2006PA001300.
Wolfe JA (1993) A method of obtaining climatic parameters from leaf assemblages. *Geological Society of America Bulletin* **2040**, 1–73.
Wu H, Guo ZT, Guiot J, Hatté C, Peng C, Yu Y, Ge J, Li Q, Sun A and Zhao D (2014) Elevation-induced climate change as a dominant factor causing the late Miocene C_4 plant expansion in the Himalayan foreland. *Global Change Biology* **20**, 1461–72.
Xing YW, Utescher T, Jacques FMB, Tao S, Liu YS, Huang YJ and Zhou ZK (2012) Palaeoclimatic estimation reveals a weak winter monsoon in southwestern China during the late Miocene: evidence from plant macrofossils. *Palaeogeography, Palaeoclimatology, Palaeoecology* **358–360**, 19–26.
Yang J, Spicer RA, Spicer TEV, Arens NC, Jacques FMB, Tao Su, Kennedy EM, Herman AB, Steart DC, Srivastava G, Mehrotra RC, Valdes PJ, Mehrotra NC, Zhou ZK and Lai JS (2015) Leaf form-climate relationships on the global stage: an ensemble of characters. *Global Ecology and Biogeography* **10**, 1113–25.
Yim S-Y, Wang B, Liu J and Wu Z (2014) A comparison of regional monsoon variability using monsoon indices. *Climate Dynamics* **43**, 1423–37.
Yin A (2006) Cenozoic tectonic evolution of the Himalayan orogen as constrained by along-strike variation of structural geometry, exhumation history, and foreland sedimentation. *Earth-Science Reviews* **76**, 1–131.
Zachos JC, Dickens GR and Zeebe RE (2008) An early Cenozoic perspective on greenhouse warming and carbon-cycle dynamics. *Nature* **451**, 279–83.
Zachos JC, Pagani M, Sloan L, Thomas E and Billups K (2001) Trends, rhythms, and aberrations in global climate 65 Ma to present. *Science* **292**, 686–93.
Zhang S and Wang B (2008) Global summer monsoon rainy seasons. *International Journal of Climatology* **28**, 1563–78.
Zhao P, Zhou XJ, Chen LX and He JH (2009) Characteristics of subtropical monsoon and rainfall over, Eastern China and Western North Pacific. *Acta Meteorologica Sinica* **23**, 649–65.

https://doi.org/10.1017/S0016756822000243 Published online by Cambridge University Press